Lithos 136–139 (2012) 93–108

Contents lists available at ScienceDirect

Lithos

journal homepage: www.elsevier.com/locate/lithos

Geochemical and U–Pb age constraints on the occurrence of polygenetic titanites in UHP metagranite in the Dabie orogen

Xiao-Ying Gao [a,*], Yong-Fei Zheng [a], Yi-Xiang Chen [a], Jingliang Guo [b]

[a] CAS Key Laboratory of Crust–Mantle Materials and Environments, School of Earth and Space Sciences, University of Science and Technology of China, Hefei 230026, China
[b] State Key Laboratory of Geological Processes and Mineral Resources, China University of Geosciences, Wuhan 430074, China

ARTICLE INFO

Article history:
Received 26 January 2011
Accepted 30 March 2011
Available online 5 April 2011

Keywords:
Titanite
UHP metamorphic rocks
U–Pb dating
Trace elements
Metamorphic growth
Continental subduction zone

ABSTRACT

Relict magmatic titanite was identified in the core of a few titanite grains with the overgrown rim of metamorphic titanite in UHP metagranite in the Dabie orogen. LA–ICPMS U–Pb dating gave Neoproterozoic ages for the magmatic titanite but Triassic ages for the metamorphic titanite. The magmatic and metamorphic titanites are clearly distinct by differences in petrological and geochemical compositions. The magmatic titanite occurs as residual cores that show bright BSE, the presence of allanite and quartz inclusions, low contents of CaO, Al_2O_3 and TiO_2 but high contents of Fe_2O_3 and MgO. In trace elements, the magmatic titanite exhibits high REE and HFSE contents, distinctly negative Eu anomalies with flat MREE–HREE patterns, and high Th/U ratios. In contrast, the metamorphic titanite occurs as rims and grains of homogeneously dark BSE that contain inclusions of epidote, quartz, K-feldspar, rutile, biotite and phengite, and have relatively high contents of CaO, Al_2O_3 and TiO_2, but low contents of Fe_2O_3 and MgO, and relatively low REE and HFSE contents, slightly negative Eu anomalies with HREE depletion relative to MREE, and low Th/U ratios. The Zr-in-titanite thermometry yields 727 to 877 °C at 0.5 to 1.0 GPa for the magmatic titanite, and 729 to 870 °C at 1.5 to 2.0 GPa for the metamorphic titanite. The Neoproterozoic U–Pb chronometric system of magmatic titanite survived the Triassic continental subduction-zone HP–UHP metamorphism. This suggests a relatively high closure temperature of >800 °C for the titanite U–Pb system. The metamorphic titanite is principally a product of retrograde metamorphism during decompression exhumation at the transition from HP eclogite-facies to amphibolite-facies. Therefore, titanite holds a great potential to geochronological and petrogenetic studies of continental subduction-zone metamorphic rocks.

1. Introduction

Titanite ($CaTiSiO_5$) is common accessory mineral that occurs in a wide range of lithology from many different geological settings (Force, 1991; Frost et al., 2000; Harlov et al., 2006). In igneous rocks, titanite is most abundant in relatively oxidized rocks with high Ca/Al ratio. In metamorphic rocks, titanite is stable to the highest temperatures in mafic and calc-silicate rocks, ranging from low to high grade metamorphic rocks. It is especially common in many high-pressure (HP) and ultrahigh-pressure (UHP) eclogite-facies rocks (e.g., Enami et al., 1993; Franz and Spear, 1985; Kylander-Clark et al., 2008) and granulite-facies rocks (Corfu et al., 1994; Dasgupta, 1993; Mezger et al., 1993; Motoyoshi et al., 1991) in continental subduction zones. Besides zircon, titanite as a common accessory mineral in igneous and metamorphic rocks has been explored recently for the purpose of geochronology and petrology.

Usually, titanite can incorporate appreciable quantities of U into its lattice (10 to >100 ppm), making titanite an important mineral for U–Pb dating (e.g., Amelin, 2009; Buick et al., 2007; Corfu et al., 1985; Corfu and Stone, 1998; Crowley, 2002; Frost et al., 2000; Li et al., 2010; Mattinson, 1986; Mattinson and Echeverria, 1980; Nemchin and Pidgeon, 1999; Pidgeon et al., 1996; Scott and St-Onge, 1995; Storey et al., 2006; Tilton and Grunenfelder, 1968; Tucker et al., 1986, 2004; Verts et al., 1996). Older and younger titanites can coexist in one rock to form linear arrays in the U–Pb concordia diagram (e.g., Tucker et al., 1986; Verts et al., 1996). A disadvantage of titanite as a geochronometric mineral is that it may contain relatively high concentrations of common Pb (Frost et al., 2000), so that analytical U–Pb isotope data require a careful assessment of the composition and proportion of the common Pb in order to make precise and accurate corrections. In general, the titanite of igneous origin contains concentrations of U up to several hundred parts per million, and only low concentrations of the common Pb so that precise U–Pb ages are often obtained. The titanite of metamorphic growth tends to contain <100 ppm U and higher proportions of the common Pb, resulting in less precise U–Pb ages and stronger dependence on the choice of initial Pb isotopic composition (Frost et al., 2000).

* Corresponding author.
E-mail address: gaoying@ustc.edu.cn (X.-Y. Gao).

0024-4937/$ – see front matter © 2011 Elsevier B.V. All rights reserved.
doi:10.1016/j.lithos.2011.03.020

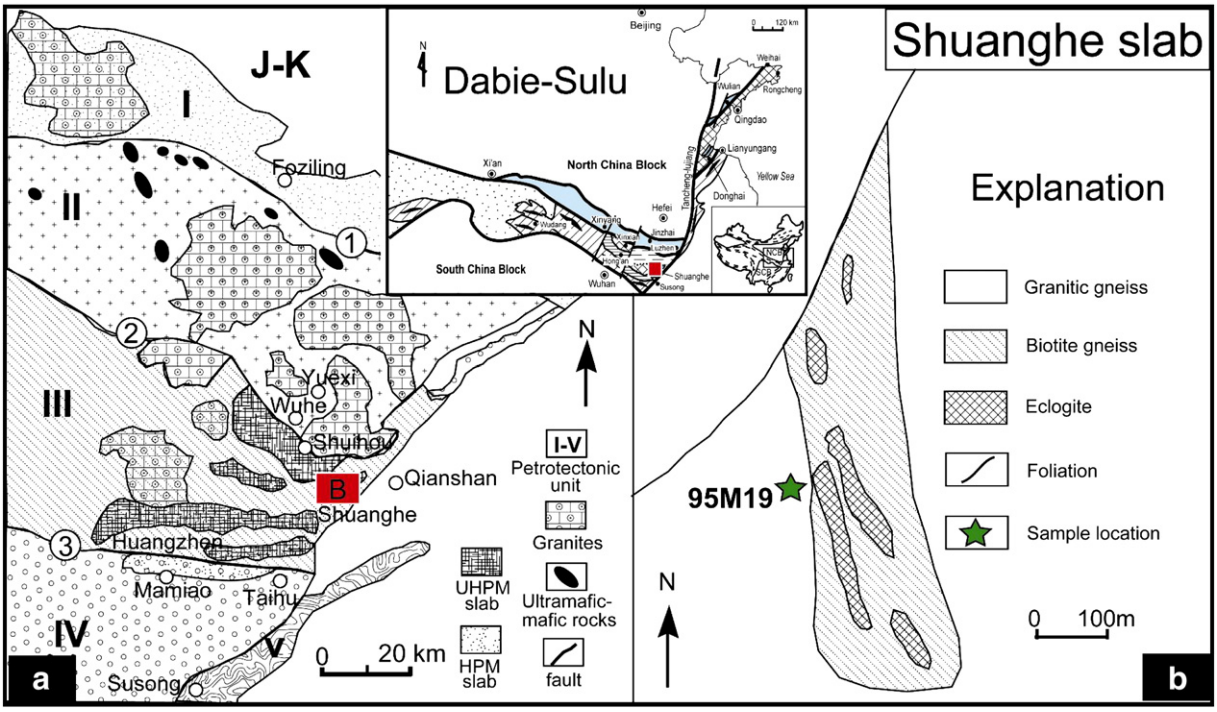

Fig. 1. Sketch geological map of the Dabie orogen and the UHP metamorphic slice at Shuanghe in Central Dabie (revised after Zheng et al., 2003b). Lithotectonic units: (I) the Beihuaiyang low-T/low-P greenschist-facies zone; (II) the North Dabie high-T/UHP granulite-facies zone; (III) the Central Dabie mid-T/UHP eclogite-facies zone; (IV) the South Dabie low-T/UHP eclogite-facies zone; (V) the Susong low-T/HP blueschist-facies zone. Circled number denotes the fault: ① Xiaotian–Mozitan Fault, ② Wuhe–Shuihou Fault, and ③ Mamiao–Taihu Fault.

Titanite has a considerable capacity for element substitutions, which makes it an important carrier of trace elements, particularly the rare earth elements (REE) and high field strength elements (HFSE). Similar to zircon, titanite can contain a large portion of REE in the rock (e.g., Buick et al., 2007; Gromet and Silver, 1983; Tiepolo et al., 2002). In contrast to zircon, titanite has chemical constituents that are major rock-forming elements. Thus, the mineral reactions that define the stability of titanite and the variable effects of pressure and temperature on solid solution compositions are reasonably well understood (Frost et al., 2000). In general, titanite occurs as a retrograde phase from rutile in eclogite and granulite during amphibolite-facies overprinting (Carswell et al., 1996; Manning and Bohlen, 1991). Based on values of X_{Al} [$=Al/(Al+Fe^{3+}+Ti)$], titanite can be divided into high-Al ($X_{Al}>0.25$) and low-Al ($X_{Al}<0.25$) varieties (Oberti et al., 1991). The

Table 1
LA–ICPMS U–Pb isotope data for titanite standards BLR-1, Khan and FCT.

Sample	Corrected ratios								Apparent age (Ma)					
	$^{207}Pb/^{206}Pb$	Error (1σ)	$^{207}Pb/^{235}U$	Error (1σ)	$^{206}Pb/^{238}U$	Error (1σ)	$^{208}Pb/^{232}Th$	Error (1σ)	$^{207}Pb/^{235}U$	Error (1σ)	$^{206}Pb/^{238}U$	Error (1σ)	$^{208}Pb/^{232}Th$	Error (1σ)
Weighted mean of $^{206}Pb/^{238}U$ ages for BLR-1: 1049 ± 7 Ma (2σ), MSWD = 1.6														
BLR-1	0.0750	0.0020	1.8181	0.0730	0.1783	0.0034	0.0581	0.0022	1052	26	1058	18	1135	41
BLR-1	0.0785	0.0019	1.9001	0.0730	0.1767	0.0032	0.0537	0.0020	1081	26	1049	18	1051	38
BLR-1	0.0735	0.0021	1.7978	0.0723	0.1756	0.0031	0.0528	0.0019	1045	26	1043	17	1034	37
BLR-1	0.0751	0.0021	1.8138	0.0713	0.1771	0.0031	0.0543	0.0018	1050	26	1051	17	1062	35
BLR-1	0.0741	0.0019	1.8645	0.0623	0.1807	0.0037	0.0594	0.0019	1069	22	1071	20	1160	36
BLR-1	0.0743	0.0020	1.8062	0.0609	0.1764	0.0036	0.0536	0.0018	1048	22	1047	20	1049	34
BLR-1	0.0746	0.0020	1.8246	0.0613	0.1760	0.0035	0.0539	0.0018	1054	22	1045	19	1055	34
BLR-1	0.0732	0.0021	1.7962	0.0632	0.1774	0.0035	0.0541	0.0019	1044	23	1053	19	1058	36
BLR-1	0.0729	0.0021	1.7700	0.0613	0.1741	0.0036	0.0531	0.0018	1035	22	1035	20	1040	34
BLR-1	0.0748	0.0020	1.8325	0.0591	0.1771	0.0036	0.0557	0.0018	1057	21	1051	20	1090	34
BLR-1	0.0730	0.0022	1.7690	0.0612	0.1726	0.0033	0.0544	0.0018	1034	22	1026	18	1065	35
BLR-1	0.0736	0.0020	1.8541	0.0613	0.1796	0.0037	0.0566	0.0019	1065	22	1065	20	1107	36
Weighted mean of $^{206}Pb/^{238}U$ ages for Khan: 510 ± 5 Ma (2σ), MSWD = 0.66														
Khan	0.0595	0.0020	0.6773	0.0304	0.0828	0.0016	0.0244	0.0009	525	18	513	9	485	18
Khan	0.0595	0.0016	0.6676	0.0254	0.0820	0.0015	0.0243	0.0008	519	15	508	9	482	16
Khan	0.0570	0.0021	0.6401	0.0293	0.0820	0.0015	0.0241	0.0009	502	18	508	9	479	17
Weighted mean of $^{206}Pb/^{238}U$ ages for FCT: 27 ± 6 Ma (2σ), MSWD = 1.8														
FCT	0.2553	0.2645	0.1999	0.1992	0.0056	0.0017	0.0019	0.0006	185	169	36	11	38	13
FCT	0.0000	0.4020	0.0000	0.1956	0.0036	0.0017	0.0009	0.0006	0	199	23	11	19	13
FCT	0.0000	0.3094	0.0000	0.1658	0.0037	0.0014	0.0013	0.0005	0	168	24	9	26	10

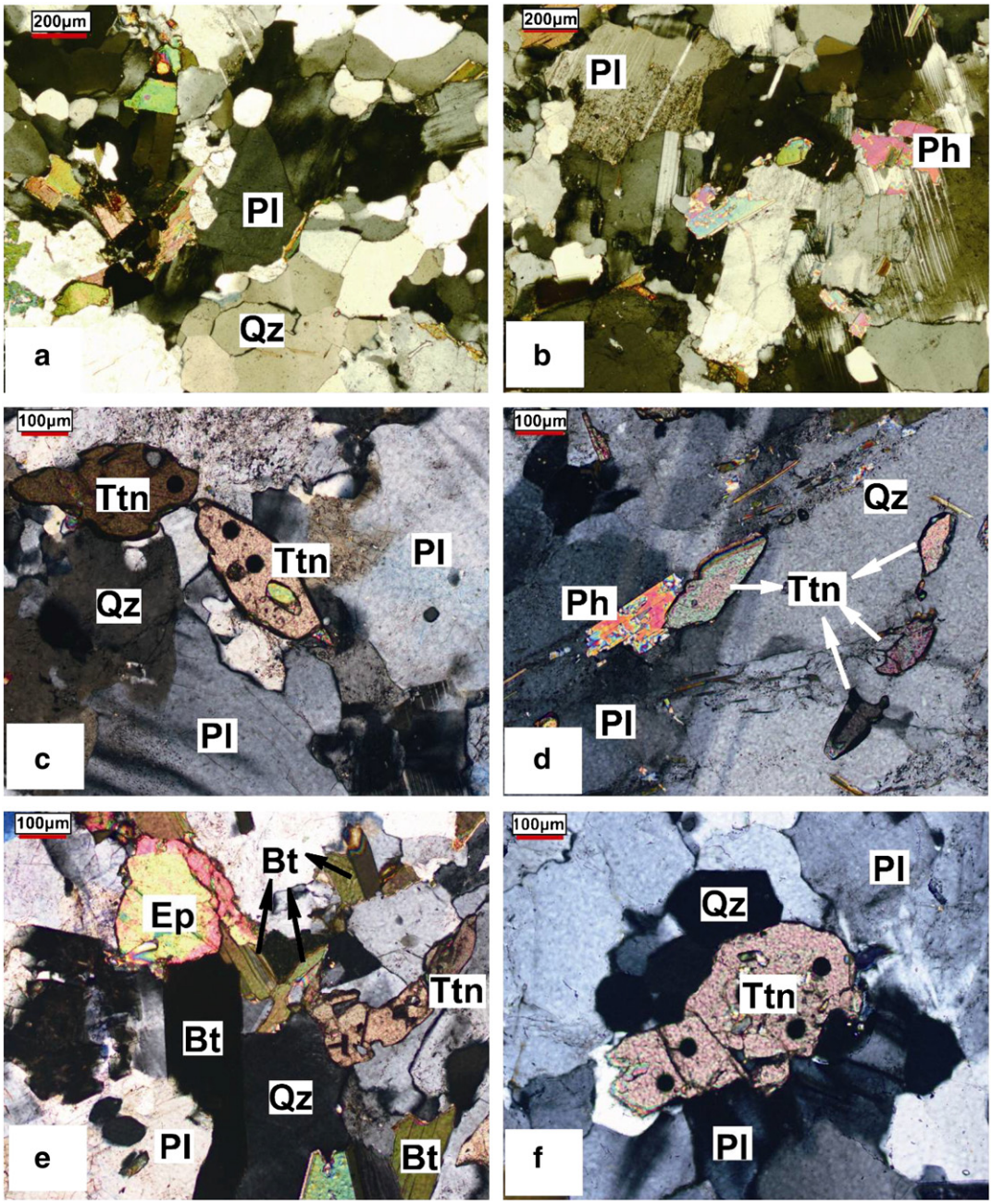

Fig. 2. Photomicrographs from UHP granitic orthogneiss at Shuanghe in the Dabie orogen (cross-polarized light). (a) and (b) Granitic gneiss composed of plagioclase, quartz and phengite. (c) to (f) Individual titanite grains as matrix minerals coexisting with different minerals.

high-Al titanite was reported in eclogite and associated rocks from a few HP metamorphic terranes (e.g., Franz and Spear, 1985; Hirajima et al., 1992; Oberti et al., 1991; Sobolev and Shatsky, 1990). It was also reported that titanite can occur as a HP phase in calc-silicate rocks and carbonate-bearing eclogites from HP or UHP terranes (Enami et al., 1993; Franz and Spear, 1985; Hirajima et al., 1992; Smith, 1977; Sobolev and Shatsky, 1990; Ye and Ye, 1996).

The substitution of Al and (F, OH) for Ti and O is very common in titanite crystal. Zirconium and Ti are important trace elements that can replace each other in crystal lattices to a limited extent. An experimental study indicates that Zr concentrations in titanite can be used as a powerful geothermometer (Hayden et al., 2008). The high-pressure experiments as well as the analyses of natural titanite crystals have established a systematic relationship between temperature, pressure and Zr concentration in titanite. The Zr-in-titanite thermometer is based on the assumption that titanite is in coexistence with rutile, zircon and quartz, so that Zr element attains thermodynamic equilibrium between them. In the system $CaTiSi_2O_5$–TiO_2–ZrO_2–SiO_2, the Zr saturation in titanite depends on activity of TiO_2 and SiO_2 as well as T and P. For HP to UHP metamorphic rocks, the pressure effect on the Zr-in-titanite thermometry cannot be ignored (Hayden et al., 2008). Thus, the Zr-in-titanite thermometer has important applicability to crustal petrology.

Titanite widely occurs in UHP metamorphic rocks in the Dabie–Sulu orogenic belt, east-central China (Carswell et al., 1996; Cong et al., 1995). These rocks have been intensively studied in perspectives of petrology, mineralogy, geochemistry and geochronology (Liou et al., 2009; Zhang et al., 2009; Zheng, 2008). The P–T conditions of various metamorphic stages and the complete P–T–t path of the eclogites have been relatively well established by petrological and

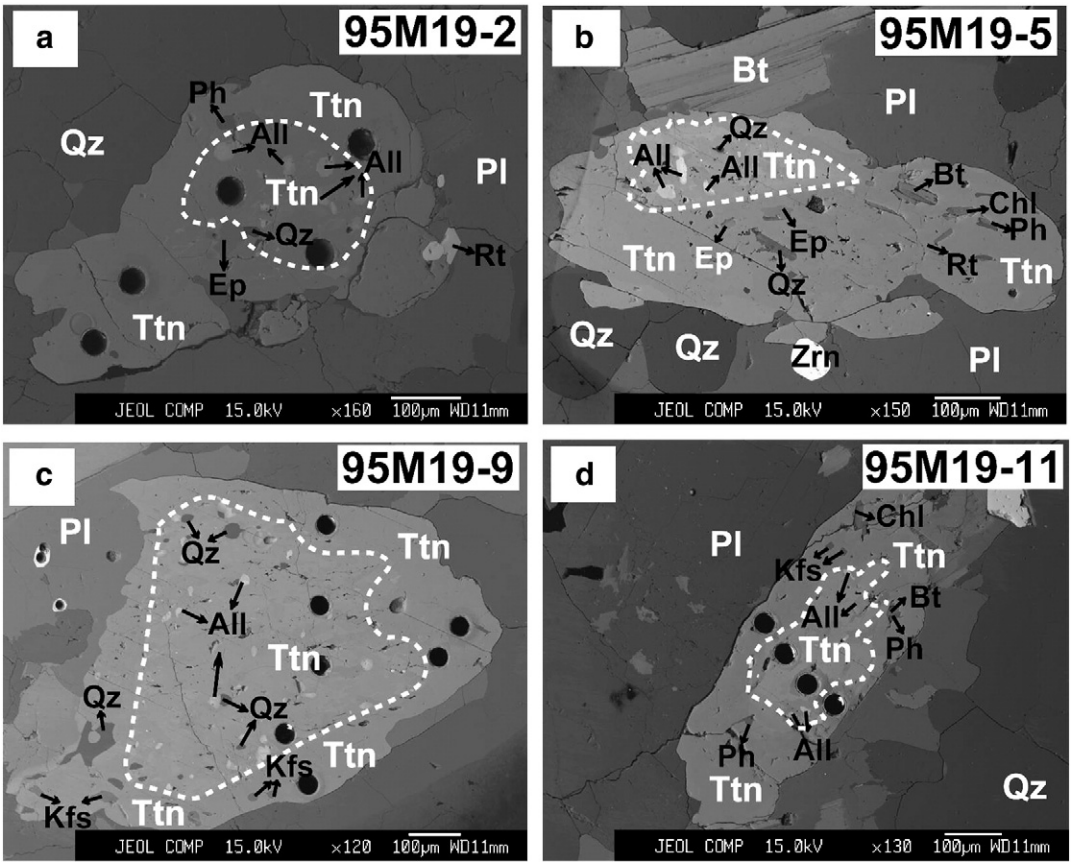

Fig. 3. Backscattered electron images showing morphological and textural features of titanite from UHP granitic orthogneiss at Shuanghe in the Dabie orogen. The round pits are laser spots. Residual cores show bright BSE with the zoned structure, whereas newly grown rims and grains exhibit homogeneously dark BSE without zoning.

geochronological studies. This provides an ideal target to explore the titanite growth during continental subduction-zone metamorphism. Based on these considerations, we have studied titanites from UHP metagranite in the Dabie orogen. Titanites of both magmatic and metamorphic origin were identified by geochemical and geochronological constraints.

2. Geological setting and samples

The Dabie–Sulu orogenic belt in east-central China was formed by the Triassic continental collision between the North China Block and the South China Block (e.g., Cong, 1996; Li et al., 1999; Liou et al., 1996; Wang et al., 1995; Zheng et al., 2003a, 2009). This belt contains

Table 2
Major element composition of inclusion minerals in titanite from granitic gneiss in the Dabie orogen.

Spot no.	Mineral	SiO_2	Na_2O	K_2O	Cr_2O_3	MgO	CaO	MnO	Al_2O_3	TiO_2	FeO	Total
19-2-1	All	33.40	0.05	0.01	–	0.12	15.88	0.67	19.74	0.33	8.68	78.87
19-2-2	All	33.55	0.02	0.01	–	0.12	14.95	0.66	18.78	0.34	9.61	78.05
19-2-3	Ph	52.16	0.16	10.46	0.01	2.66	0.21	0.09	26.15	0.83	6.23	98.97
19-2-4	Ep	38.03	0.02	0.02	–	0.06	22.80	0.29	21.47	0.28	13.22	96.18
19-5-1	All	30.56	0.04	0.03	–	0.31	11.16	0.80	12.71	0.57	15.82	72.01
19-5-2	All	33.56	0.04	0.01	–	0.17	15.36	0.52	17.58	0.37	12.39	80.00
19-5-3	Qz	98.70	–	0.02	–	0.01	0.24	–	0.07	0.37	0.03	99.44
19-5-4	Bt	36.35	0.13	9.65	0.05	9.78	0.24	0.84	15.46	1.09	23.85	97.42
19-5-5	Chl	24.49	0.35	0.39	0.12	11.11	0.42	1.79	16.00	0.62	31.38	86.66
19-5-6	Ph	50.68	0.18	9.91	0.05	2.27	0.28	0.12	26.56	0.82	6.94	97.80
19-5-7	Chl	26.75	0.27	0.27	0.90	12.31	0.55	1.78	16.60	0.78	28.08	88.29
19-5-8	Ep	37.70	0.02	0.02	–	0.04	22.31	0.65	18.53	0.33	16.49	96.10
19-9-1	All	31.97	0.04	0.03	–	0.26	13.71	0.82	14.42	0.64	15.58	77.46
19-9-2	All	31.48	0.01	0.00	–	0.24	13.38	0.53	14.68	0.39	14.57	75.28
19-9-3	All	31.14	–	0.01	–	0.26	13.11	0.54	14.30	0.53	14.80	74.69
19-9-4	Kfs	63.95	0.43	15.54	–	0.02	0.08	–	18.03	0.21	0.03	98.29
19-9-5	Kfs	63.94	0.71	15.44	0.01	0.03	0.21	–	17.89	0.31	0.01	98.54
19-11-0	Chl	25.75	0.29	0.29	0.11	11.31	0.57	1.78	16.40	0.73	29.08	86.31
19-11-2	Bt	35.17	0.17	9.82	0.12	8.79	0.45	0.76	14.04	2.30	25.20	96.81
19-11-3	Ph	50.14	0.10	10.29	–	2.64	0.18	0.09	24.53	0.65	8.91	97.52
19-11-4	Ph	50.59	0.22	10.29	0.02	2.13	0.23	0.07	25.56	0.76	7.39	97.26

Note: The element contents below the detection limit of electron microprobe analyses are denoted as "–"; Mineral abbreviations are after Whitney and Evans (2010): All — allanite, Ph — phengite, Ep — epidote, Qz — quartz, Bt — biotite, Chl — chlorite, and Kfs — K-feldspar.

one of the largest (>30,000 km^2) and best-exposed UHP metamorphic terranes recognized so far on Earth (Carswell and Compagnoni, 2003; Ernst, 2005; Zheng, 2008). Findings of coesite and microdiamond as inclusions in minerals from the Dabie–Sulu metamorphic rocks led to the recognition of UHP metamorphism and continental deep subduction in east-central China (Okay et al., 1989; Wang et al., 1989, 1992; Xu et al., 1992, 2003, 2005). A lot of studies of mineralogy and petrology have demonstrated that the metamorphic rocks from the Dabie–Sulu orogenic belt underwent UHP metamorphism at temperatures of 700 to 800 °C and pressures of 2.8 to 3.6 GPa (Liou et al., 2009; Zhang et al., 2009).

The Dabie orogen is a major segment consisting of a series of fault-bounded metamorphic units (Fig. 1). From north to south, it can be divided into five zones based on the lithotectonic characteristics (Zheng, 2008; Zheng et al., 2005a): (1) the Beihuaiyang low-T/low-P greenschist-facies zone, which consists of slate, phyllite, metasandstone, schist and metaigneous rocks of mainly greenschist-facies dynamic metamorphism and is overlain by Jurassic–Cretaceous molasse-like sedimentary and volcanic rocks; (2) the North Dabie high-T/UHP granulite-facies zone with migmatization, which consists of abundant amphibolite-facies to granulite-facies rocks as well as some migmatitic gneisses and a few mafic–ultramafic complexes, and Mesozoic granitic rocks;(3) the Central Dabie mid-T/UHP eclogite-facies zone, which consists of coesite-bearing eclogites, gneisses, marbles, jadeite quartzites, and minor ultramafic rocks; (4) the South Dabie low-T/UHP eclogite-facies zone, which consists mainly of epidote/amphibolite-facie rocks with a few low-T eclogites, and (5) the Susong low-T/HP blueschist-facies zone.

In general, three metamorphic stages have been recognized for the mid-T/UHP metamorphic rocks in the Dabie–Sulu orogenic belt (Cong et al., 1995; Gao et al., 2011; Liou et al., 2009; Zhao et al., 2006; Zheng et al., 2003a, 2011): (1) peak UHP coesite eclogite-facies, which is recorded by coesite and jadeite-rich omphacite inclusions in garnet. Metamorphic temperatures range from about 800 to 700 °C at >2.8 GPa; (2) HP quartz eclogite-facies recrystallization, which is represented by the coexistence of garnet and omphacite with quartz instead of coesite. Metamorphic conditions were estimated to range from about 850–750 °C at 2.5–2.0 GPa to 650–600 °C at 2.0–1.0 GPa; (3) amphibolite-facies retrogression, which is indicated by the occurrence of various symplectites such as amphibole + sodic plagioclase after omphacite in eclogite. Temperature and pressure conditions of this stage were estimated to be about 600 to 450 °C and 1.0 to 0.6 GPa. Usually, the granitic orthogneiss (metagranite) is a poor recorder of UHP metamorphism because UHP index minerals are susceptible to retrogression and UHP paragenesis is frequently reequilibrated at amphibolite-facies conditions due to the presence of hydrous minerals (e.g., Chen et al., 2011; Liu and Liou, 2011; Tsai and Liou, 2000; Xiao et al., 2001; Zhang et al., 1995; Zheng et al., 2003b).

This study focuses on UHP metamorphic rocks at Shuanghe in the eastern part of the Dabie orogen, which belongs to the mid-T/UHP eclogite-facies zone (Fig. 1). It is located in Qianshan Country, Anhui province. As demonstrated by Cong et al. (1995), Carswell et al. (1997) and Fu et al. (1999), the UHP eclogite slice at Shuanghe was separated into two units by a dextral strike–slip fault. Both units, with outcrop area about 1 km^2, are surrounded by the UHP granitic orthogneiss. Previous studies have examined the petrology, mineralogy, geochemistry and geochronology of UHP metamorphic rocks in this locality (e.g., Carswell et al., 1997; Cong et al., 1995; Fu et al., 1999, 2001; Gao et al., 2011; Li et al., 2000; Liu et al., 2006; Okay, 1993; Wu et al., 2006; Zhang et al., 2003; Zheng et al., 1998, 2000, 2003b). The eclogites at Shuanghe occur as not only small lenses and enclaves within, but also as large-scale blocks interlayered with, the granitic orthogneiss, biotite paragneiss and marble. The biotite paragneiss commonly occurs as compositional layers with the eclogite, marble and jadeite quartzite. Coesite and its pseudomorph

Table 3
LA–ICPMS trace element and U–Pb isotope data for titanite from granitic orthogneiss in the Dabie orogen.

Spot	Rb (ppm)	Sr (ppm)	Zr (ppm)	Nd (ppm)	Sm (ppm)	Lu (ppm)	Hf (ppm)	Pb (ppm)	Th (ppm)	U (ppm)	Corrected ratios								Apparent age (Ma)							
											$^{207}Pb/^{206}Pb$	Error (1σ)	$^{207}Pb/^{235}U$	Error (1σ)	$^{206}Pb/^{238}U$	Error (1σ)	$^{208}Pb/^{232}Th$	Error (1σ)	$^{207}Pb/^{235}U$	Error (1σ)	$^{206}Pb/^{238}U$	Error (1σ)	$^{208}Pb/^{232}Th$	Error (1σ)
1	2.20	323	734	6276	1836	259	75.1	34.7	162	71.9	0.0645	0.0044	0.7968	0.0620	0.0896	0.0026	0.0332	0.0021	595	61	553	16	758	145
2	1.07	457	31.1	765	387	24.2	2.73	16.0	12.6	64.3	0.0507	0.0035	0.2372	0.0185	0.0339	0.0010	0.0595	0.0037	216	19	215	6	229	158
3	0.39	756	50.2	1052	456	24.2	8.07	19.4	24.4	75.0	0.0505	0.0035	0.2393	0.0184	0.0344	0.0010	0.0035	0.0002	218	19	218	7	216	159
4	0.39	839	107	453	159	31.4	27.6	24.8	18.5	32.3	0.0786	0.0054	0.3566	0.0286	0.0329	0.0010	0.0671	0.0042	310	29	209	6	1162	135
5	0.56	724	89.2	1815	666	34.8	37.8	25.3	48.1	78.5	0.0555	0.0038	0.2571	0.0197	0.0336	0.0010	0.0189	0.0013	232	20	213	6	433	152
6	2.83	481	99.1	1688	155	21.7	28.5	32.3	27.7	55.7	0.0517	0.0035	0.2486	0.0197	0.0349	0.0010	0.0493	0.0031	225	20	221	7	270	156
7	2.38	832	101	1483	149	47.4	23.1	30.7	23.9	63.1	0.0652	0.0044	0.3064	0.0235	0.0341	0.0010	0.0386	0.0024	271	24	216	6	780	143
8	3.29	377	990	8922	2497	276	115	50.6	322	136.	0.0656	0.0045	1.0203	0.0764	0.1128	0.0032	0.0356	0.0023	714	75	689	21	794	143
9	2.85	440	846	7427	2145	224	92.1	39.7	213	113	0.0650	0.0046	0.8819	0.0734	0.0984	0.0030	0.0317	0.0020	642	72	605	19	774	147
10	0.35	1103	24.3	1236	502	14.5	2.95	19.9	34.8	46.7	0.0533	0.0038	0.2565	0.0205	0.0349	0.0012	0.0388	0.0027	232	21	221	7	342	160

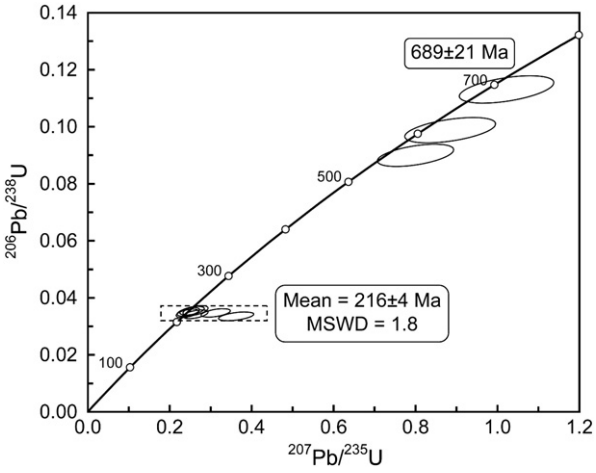

Fig. 4. Cumulative probability plot of titanite U–Pb ages from UHP granitic orthogneiss at Shuanghe in the Dabie orogen.

were observed in both garnet and dolomite from these UHP metamorphic rocks (e.g., Schertl and Okay, 1994; Wang et al., 1989; Wang and Liou, 1991). Petrological studies suggest that the peak metamorphic pressures for the UHP eclogites are greater than 3.0 GPa at temperature of 700 to 800 °C based on the garnet-clinopyroxene Fe–Mg partition geothermometry (Carswell et al., 1997; Cong et al., 1995; Okay, 1993).

The sample used in this study is a metagranite (granitic orthogneiss) that encloses the UHP eclogite of the lower unit at Shuanghe (Fig. 1). The hydrogen, oxygen, carbon and hafnium isotope compositions of mineral separates and whole-rock were studied in detail by Fu et al. (1999) and Zheng et al. (2003b, 2005b, 2006). Zircon U–Pb dating has obtained that the gneiss has the Triassic metamorphic ages of 215 ± 17 to 228 ± 12 Ma and Neoproterozoic protolith ages of 724 ± 22 to 768 ± 22 Ma (Zheng et al., 2003b, 2005b, 2006).

3. Analytical method

Mineral inclusions in titanite were analyzed quantitatively by wave dispersive X-ray spectrometer (WDS) or qualitatively by energy dispersive X-ray spectrometer (EDS) on the JEOL JXA-8100 electronic microprobe (EMP) at the State Key Laboratory of Geological Processes and Mineral Resources in China University of Geosciences, Wuhan. BSE images were obtained by EDS using the same EMP. Operating conditions were set at 15 kV for accelerating voltage and 20 nA for beam current. The relative lightness of individual BSE images reflects image-specific variations in average atomic weight. In general, darker areas correspond to relatively lower average atomic weights, whereas bright areas correspond to relatively higher average atomic weights. However, it should be noted that the lightness difference between BSE images for different titanite grains may reflect the contrast during operation, not necessarily the chemical difference.

Trace element and U–Pb isotope analyses of titanite were performed separately on thin sections (~50 μm thick) by the in-situ LA–ICPMS (laser ablation inductively coupled mass spectrometry) method at State Key Laboratory of Geological Processes and Mineral Resources

Table 4
Major elements in titanite from granitic orthogneiss in the Dabie orogen.

Spot[a]	TiO_2	CaO	SiO_2	Al_2O_3	Fe_2O_3	Na_2O	Na_2O	MgO	P_2O_5	K_2O	MnO	X_{Al}
1-1n	33.4	29.9	29.8	4.82	0.25	0.05	0.05	0.01	0.01	bdl	0.05	0.18
1-2n	33.0	30.1	29.9	5.44	0.27	0.07	0.07	0.01	0.01	bdl	0.13	0.20
1-3n	33.2	29.6	30.1	5.01	0.26	0.06	0.06	0.01	0.01	bdl	0.07	0.19
5-1-core	31.6	26.0	28.5	2.45	3.70	0.09	0.09	0.30	0.02	bdl	0.32	0.10
5-2-core	32.6	26.9	29.5	3.59	1.83	0.10	0.10	0.09	0.02	bdl	0.16	0.14
5-3-core	30.9	26.4	29.3	4.20	3.18	0.10	0.10	0.12	0.03	bdl	0.24	0.16
5-4-rim	33.0	29.8	29.9	5.44	0.40	0.07	0.07	0.01	0.01	bdl	0.12	0.20
5-5-rim	33.1	29.9	30.0	5.33	0.50	0.05	0.05	0.01	0.01	bdl	0.13	0.20
7-1n	32.9	29.3	29.5	5.33	0.87	0.06	0.06	0.02	0.02	0.01	0.14	0.20
8-1n	32.6	29.6	29.9	5.79	0.46	0.05	0.05	0.01	0.01	bdl	0.15	0.22
8-2n	32.1	28.9	30.9	5.29	0.54	0.07	0.07	0.03	0.02	bdl	0.13	0.20
8-3n	33.3	29.9	29.2	5.79	0.27	0.06	0.06	0.01	0.01	bdl	0.09	0.21
9-1-rim	32.3	30.3	30.2	5.33	0.25	0.06	0.06	bdl	0.01	bdl	0.08	0.2
9-2-rim	33.1	29.9	30.0	4.27	0.46	0.06	0.06	0.01	0.02	bdl	0.09	0.17
9-3-rim	33.3	30.5	29.9	4.07	1.11	0.06	0.06	0.03	0.02	0.04	0.16	0.16
9-4-core	30.9	27.3	30.1	3.99	1.87	0.08	0.08	0.09	0.03	bdl	0.15	0.16
9-5-core	31.6	27.5	28.9	3.86	2.23	0.12	0.12	0.12	0.05	bdl	0.18	0.15
9-6-core	32.4	27.4	29.0	4.24	1.64	0.12	0.12	0.05	0.04	bdl	0.16	0.16
9-7-rim	32.6	30.3	30.1	4.88	0.69	0.07	0.07	0.01	0.03	bdl	0.14	0.19
11-1-rim	33.3	29.5	29.9	5.39	0.28	0.06	0.06	0.01	0.01	bdl	0.07	0.20
11-2-core	32.1	28.3	29.4	4.02	1.70	0.09	0.09	0.11	0.02	bdl	0.19	0.16
11-3-core	30.7	26.6	28.9	2.31	3.80	0.12	0.12	0.29	0.04	bdl	0.33	0.09
11-4-core	30.8	26.3	28.9	2.47	3.86	0.11	0.11	0.30	0.04	bdl	0.33	0.10
14-1n	31.6	30.5	30.3	5.36	0.65	0.05	0.05	0.01	0.02	bdl	0.11	0.21
14-2n	33.2	30.5	29.3	4.86	0.51	0.06	0.06	0.05	0.02	0.10	0.13	0.18
14-3n	32.8	30.8	29.4	5.50	0.29	0.05	0.05	0.01	0.01	bdl	0.13	0.21
15-2n	33.2	29.4	30.2	5.21	0.26	0.06	0.06	0.01	0.01	bdl	0.05	0.20
15-3n	32.1	30.9	29.6	5.51	0.41	0.06	0.06	0.03	0.02	bdl	0.13	0.21
18-2n	31.5	30.9	30.3	5.12	0.40	0.06	0.06	0.04	0.01	bdl	0.10	0.2
19-1n	33.9	29.9	29.1	5.08	0.41	0.05	0.05	0.01	0.02	bdl	0.11	0.19
22-1n	33.2	30.5	28.9	5.29	0.30	0.05	0.05	0.01	0.01	bdl	0.09	0.20
22-2n	31.1	31.4	30.3	5.39	0.28	0.06	0.06	bdl	bdl	bdl	0.07	0.21
22-3n	31.2	30.8	31.1	5.02	0.35	0.07	0.07	0.01	0.01	0.01	0.09	0.2
22-4n	30.5	31.4	30.6	5.73	0.25	0.06	0.06	bdl	0.01	bdl	0.07	0.23
25-1n	31.4	30.9	30.7	4.92	0.20	0.06	bdl	bdl	bdl	0.09	0.29	0.20

Notes: [a]n denotes the homogenous titanite grains; "bdl" denotes the contents below the detection limit.

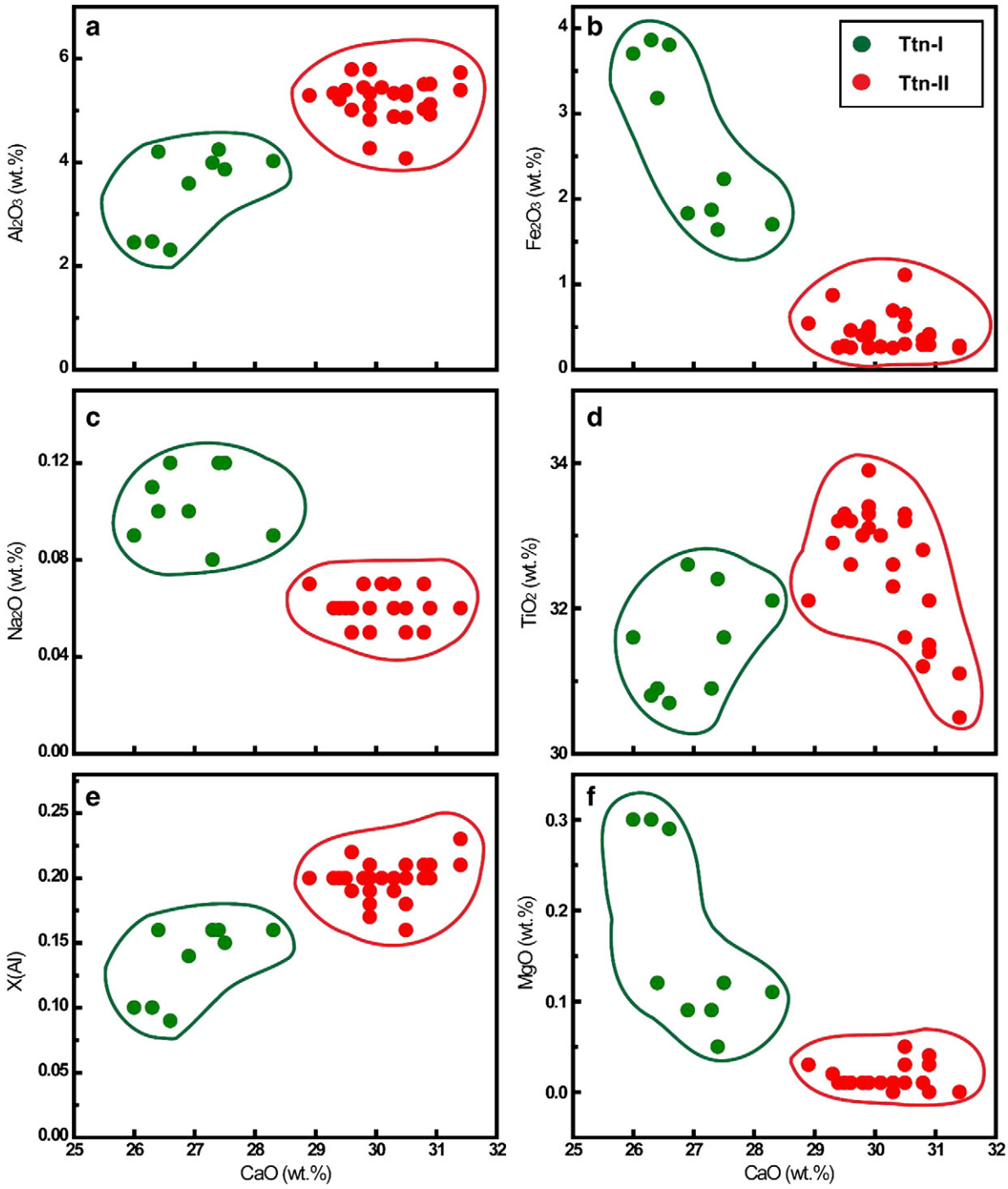

Fig. 5. Plots of CaO vs. other major elements for two groups of titanites from UHP granitic orthogneiss at Shuanghe in the Dabie orogen. Ttn-I domains denote the residual cores, and Ttn-II domains denote the newly grown rims or grains.

in China University of Geosciences, Wuhan. Detail analytical protocols and data reduction method for trace elements were presented by Liu et al. (2008, 2010). The laser ablation system was a GeoLas 2005, which was equipped with a 193 nm ArF excimer laser and a homogenizing optical imaging system (GeoLas 2005). An Agilent 7500a ICP-MS instrument was used to acquire ion-signal intensities. The Agilent ChemStation was utilized for the acquisition of each individual analysis.

Laser ablation spots of the trace element analysis of titanite were set to be 32 μm, with the laser energy of 60 mJ and a frequency of 5 Hz. The isotopes measured are ^{25}Mg, ^{27}Al, ^{29}Si, ^{49}Ti, ^{51}V, ^{53}Cr, ^{57}Fe, ^{63}Cu, ^{66}Zn, ^{88}Sr, ^{91}Zr, ^{93}Nb, ^{121}Sb, ^{178}Hf, ^{181}Ta, ^{182}W and ^{238}U. Four standard materials, USGS glasses GSE-1G, BCR-2G, BHVO-2G and BIR-1G, were used for multiple-standard calibration. Off-line selection and integration of background and analyte signals, and time-drift correction and quantitative calibration were conducted by the EXCEL-based software ICPMSDataCal (Liu et al., 2008, 2010). Reproducibility and accuracy of trace element concentrations were assessed to be better than ±5% for major elements and better than ±5–10% for most trace elements based on repeated analyses of the reference materials. To acquire reliable trace element concentrations, the time-resolved spectrum of every element for every sample was carefully

Table 5
Trace elements in titanite from granitic orthogneiss in the Dabie orogen.

Spot	1-1n	1-2n	1-3n	5-1-core	5-2-core	5-3-core	5-4-rim	5-5-rim	7-1n	8-1n	8-2n
Rare earth elements (ppm)											
La	429	36	344	1949	657	1492	75	219	148	172	340
Ce	2118	226	1771	7935	3692	6549	479	1030	827	935	1657
Pr	456	62	395	1494	887	1286	125	202	204	219	374
Nd	2587	441	2289	7874	5432	6930	870	1116	1313	1380	2238
Sm	772	270	721	2337	1868	2070	444	330	529	527	801
Eu	215	87.9	198	121	127	108	132	102	149	150	167
Gd	732	442	729	2609	2096	2196	623	357	694	605	917
Tb	114	103	120	499	410	410	122	64	147	107	163
Dy	631	733	700	3386	2818	2728	801	408	1099	684	1013
Ho	106	142	121	739	591	570	154	81	225	129	190
Er	250	369	298	2347	1866	1768	411	225	603	352	503
Tm	29.2	45.4	35.8	357.2	274.1	257.2	52.1	31.4	73.8	43.4	63.3
Yb	160	253	198	2359	1768	1632	287	196	414	259	366
Lu	15.6	23.3	19.4	264.2	194.5	171.4	28.2	23.3	38.7	27.5	37.1
REE	8616	3233	7939	34,271	22,681	28,168	4605	4385	6465	5591	8831
Trace elements (ppm)											
Sr	1383	205	1070	125	749	388	496	1054	835	895	1077
Ta	46.4	67.5	54.9	231.5	159.0	250.2	62.6	23.0	94.9	104.7	94.6
Nb	817	1154	944	2157	2010	2288	1004	556	1405	1049	1216
Th	71.0	4.5	67.6	165.7	67.6	134.0	13.8	43.9	44.3	35.3	74.4
U	56.4	39.7	66.8	95.9	71.4	52.4	64.7	39.8	66.7	58.8	83.6
Pb	54.0	13.2	47.5	21.4	46.6	34.9	15.8	29.4	24.4	23.0	31.6
Zr	30.7	37.0	33.5	935	213	441	35.8	78.6	38.8	50.0	107
P	40.2	60.6	49.5	102.7	84.9	122.6	46.5	28.8	72.2	61.4	66.7
Y	2831	3921	3288	21,394	16,927	16,141	4211	2365	6482	3660	5278
Hf	2.08	2.94	2.64	113.25	30.83	65.45	3.05	14.02	3.23	5.07	9.92
V	18.3	10.1	13.4	115.9	106.9	117.1	17.0	97.7	64.7	53.9	25.1
W	5.87	1.09	4.96	1.59	1.73	1.12	1.87	6.90	2.55	5.42	3.33
Lu/Hf	7.48	7.92	7.36	2.33	6.31	2.62	9.24	1.67	11.97	5.42	3.74
Nb/Ta	17.62	17.10	17.20	9.32	12.64	9.14	16.04	24.14	14.81	10.02	12.86
Eu/Eu*	0.88	0.78	0.84	0.15	0.20	0.16	0.77	0.91	0.75	0.81	0.59
$(Gd/Lu)_N$	5.83	2.36	4.66	1.23	1.34	1.59	2.75	1.90	2.23	2.73	3.07

Note: $Eu/Eu^* = Eu_N/\sqrt{Sm_N{}^*Gd_N}$, where N denotes normalization to chondrite values after Sun and McDonough (1989).

examined. If significant spikes or fluctuations were observed in the time-resolved spectrum for some elements, the concentration of this element would be considered unreliable and thus discarded for further study.

Laser ablation spots of U–Pb dating were set to be 60 μm, with the laser energy of 60 mJ and a frequency of 6 Hz. The isotopes measured are ^{201}Hg, ^{202}Hg, $^{204}(Hg+Pb)$, ^{206}Pb, ^{207}Pb, ^{208}Pb, ^{232}Th, ^{235}U and ^{238}U. The interference of ^{204}Hg for ^{204}Pb intensity was eliminated by calculated ^{204}Hg from the natural abundance of Hg isotopes with $^{204}Hg/^{201}Hg = 0.521$ (Zadnik et al., 1989) and measured ^{201}Hg intensity (Horstwood et al., 2003; Storey et al., 2006). Thus, common lead could be corrected by applying the ^{204}Pb and common lead composition calculated from the two-stage terrestrial lead isotope evolution model of Stacey and Kramers (1975). Uncertainties of the corrected U–Pb ages were propagated from the ^{201}Hg, $^{204}(Pb+Hg)$, ^{206}Pb, ^{207}Pb, ^{208}Pb, ^{232}Th and ^{238}U intensities processed by ICPMSDataCal (Liu et al., 2008, 2010). Three standard titanites, BLR-1, Khan and FCT, were utilized in this study (Table 1). Titanite BCL-1 was used as the reference and repeated analyses gave a weighted mean of U–Pb ages at 1049 ± 7 Ma (2σ, n = 12). This age is consistent with a recommended $^{206}Pb/^{238}U$ age of 1047 ± 1 Ma (Aleinikoff et al., 2007). Titanites Khan and FCT were used as unknowns for test. A weighted mean of $^{206}Pb/^{238}U$ ages for titanite Khan is 510 ± 5 Ma (2σ, n = 3), which is ~2% younger than, but still consistent within errors with, reported $^{206}Pb/^{238}U$ ages of 518–522 Ma (Heaman, 2009; Kinny et al., 1994). For titanite FCT, a weighted mean of $^{206}Pb/^{238}U$ ages is 27 ± 6 Ma (2σ, n = 3), which is also identical to a reported $^{206}Pb/^{238}U$ age of 28.395 ± 0.049 Ma (Schmitz and Bowring, 2001).

The abbreviation of minerals in this paper is after Whitney and Evans (2010).

4. Results

4.1. Petrography and inclusions in titanite

The present study focuses on granitic orthogneiss 95 M19. It consists of plagioclase, quartz, phengite, biotite, and epidote with such accessory minerals as garnet, titanite and/or rutile, ilmenite and magnetite. Titanite from the metagranite occurs mostly as euhedral to subhedral grains (Fig. 2). Crystals are yellow brown to pale, and 50–1000 μm in diameter. The large titanites commonly contain abundant small inclusions (Fig. 3). Titanite grains are homogeneous in transmitted light, but BSE images show internal zoning for a few titanites.

Different domains of core and rim can be recognized by the lightness difference between BSE images for titanite on thin sections. Most titanites are relatively homogeneous with indiscernible lightness in BSE, but a few grains show compositional zoning with a brighter core and a darker rim. The zoned grains are euhedral to subhedral, dark brown crystals in sizes of 200–1000 μm. The cores are denoted by Ttn-I domains whereas the rims and grains of homogeneously dark BSE are denoted as Ttn-II domains. Mineral inclusions of allanite and quartz occur in the cores of bright BSE. On the other hand, mineral inclusions of epidote, biotite, chlorite, phengite, quartz, rutile and K-feldspar were found in the rims and grains of homogeneously dark BSE (Fig. 3). Table 2 lists the major element compositions of inclusion minerals.

4.2. U–Pb geochronology

Titanite U–Pb isotope results are listed in Table 3. Overall 25 LA–ICMPS analyses of titanites were performed on a thin section, and 15

8-3n	S9-1-rim	9-2-rim	9-3-rim	9-4-core	9-5-core	9-6-core	9-7-rim	11-1-rim	11-2-core	11-3-core	11-4-core
108	148	478	34	1143	859	839	118	222	965	2483	2409
638	925	2461	245	4671	3821	3693	712	1234	4142	10,099	9822
165	223	544	69	935	876	790	160	296	852	1753	1672
1135	1437	3008	502	4844	4799	4412	1029	1864	4489	8620	8404
521	592	926	315	1542	1751	1565	490	663	1492	2376	2302
148	161	219	108	103	88.1	92.0	134	182	137	105	97.7
671	733	923	495	1798	2152	1950	658	708	1762	2588	2618
126	114	132	82.7	310	403	356	110	118	298	432	432
806	742	817	520	2288	3077	2735	748	693	2154	3114	3221
151	134	145	83.9	486	669	579	134	120	443	669	675
392	355	379	190	1541	2153	1853	340	298	1364	2155	2148
48.0	38.6	44.7	19.8	206	295	252	37.8	34.6	181	291	297
268	213	254	108	1274	1835	1533	216	191	1113	1864	1865
27.1	22.5	27.8	11.5	152	212	178	21.8	19.3	129	231	235
5204	5840	10,359	2784	21,292	22,989	20,825	4909	6642	19,522	36,780	36,199
705	974	1134	543	836	824	1006	545	1247	675	128	128
62.8	67.4	84.3	85.9	85.8	132.4	130.7	68.8	60.1	176.8	274.3	220.7
1007	1010	1102	1226	1357	2626	2821	1059	955	2014	2652	2404
21.7	30.2	65.2	4.8	113.2	99.8	116.3	19.8	68.8	75.4	209.6	214.8
74.3	83.1	49.6	30.7	74.7	62.5	58.9	67.0	82.3	61.7	118.2	123.9
15.7	21.8	45.4	17.0	34.0	54.4	49.9	24.4	32.0	25.2	23.9	27.6
33.4	32.1	50.1	47.5	238.1	479.1	212.8	47.2	35.9	351.3	954.1	942.3
36.8	50.7	71.7	84.1	115.4	214.8	181.7	127.0	41.3	82.3	170.5	176.9
4142	3552	3722	2265	13,384	19,096	16,091	3520	3317	12,170	18,978	18,884
2.58	2.60	5.48	4.95	31.39	56.47	28.38	4.02	2.88	41.05	106.73	101.86
12.3	11.5	31.3	58.7	105.4	113.2	99.2	25.7	13.4	99.7	110.6	114.8
1.77	2.54	6.64	1.51	1.66	1.87	1.75	1.51	3.08	4.34	2.37	2.77
10.49	8.65	5.07	2.32	4.85	3.75	6.27	5.42	6.71	3.15	2.16	2.31
16.04	14.99	13.08	14.26	15.81	19.84	21.58	15.40	15.89	11.39	9.67	10.90
0.77	0.75	0.72	0.84	0.19	0.14	0.16	0.72	0.81	0.26	0.13	0.12
3.08	4.05	4.13	5.36	1.47	1.26	1.36	3.75	4.55	1.69	1.39	1.38

of them contain very high common Pb compositions and thus were discarded for further discussion. The remaining ten U–Pb analyses gave two groups of ages (Fig. 4). An older group has Neoproterozoic $^{206}Pb/^{238}U$ ages of 553 ± 17 to 689 ± 21 Ma for the cores of bright BSE. And a distinctly younger group has Triassic $^{206}Pb/^{238}U$ ages of 209 ± 6 Ma to 221 ± 7 Ma for the rims and grains of homogeneously dark BSE, yielding a weighted mean of 216 ± 4 Ma at 2σ error (MSWD = 1.8).

The older group of U–Pb ages was all obtained from domains Ttn-I, so that the oldest age of 689 ± 21 Ma may approximately date the crystallization of protolith titanite. In contrast, the younger group was all obtained from domains Ttn-II, and their U–Pb ages likely date the growth of metamorphic titanite. There are no Paleozoic U–Pb ages on domains Ttn-I, suggesting neither mixing of sampling domains Ttn-I and Ttn-II, nor significant recrystallization of protolith titanite to cause profound loss of radiogenic Pb during the Triassic subduction-zone metamorphism.

4.3. Major and trace elements of titanite

The major element results of titanite are presented in Table 4 and Fig. 5, and the trace element results are presented in Table 5 and Figs. 6 and 7. A total of 37 analyses on 13 titanite grains were performed by LA–ICPMS. In general, domains Ttn-I are chemically distinct from domains Ttn-II as shown by pronounced differences in Al_2O_3, CaO and TiO_2 (Table 4) and their overall variation in trace element abundance (Table 5).

Domains Ttn-I have relatively uniform contents of SiO_2 (28.5 to 30.1 wt.%), TiO_2 (30.7 to 32.6 wt.%), CaO (26.0 to 28.3 wt.%), Al_2O_3 (2.31 to 4.24 wt.%), and Fe_2O_3 (1.64 to 3.68 wt.%). Mole fractions of aluminum (X_{Al}) in these domains are 0.09 to 0.16 (Table 4), with an average of 0.14. Domains Ttn-II also have relatively uniform contents for SiO_2 (28.9 to 31.1 wt.%), TiO_2 (30.5 to 33.9 wt.%), CaO (28.9 to 31.4 wt.%), Al_2O_3 (4.07 to 5.79 wt.%), and Fe_2O_3 (0.25 to 1.11 wt.%). Their X_{Al} values are 0.16 to 0.23 with an average of 0.20. Nevertheless, the groups of domains are distinguishable from each other in diagrams of CaO vs. Al_2O_3, Na_2O, MgO, Fe_2O_3 and TiO_2 (Fig. 5).

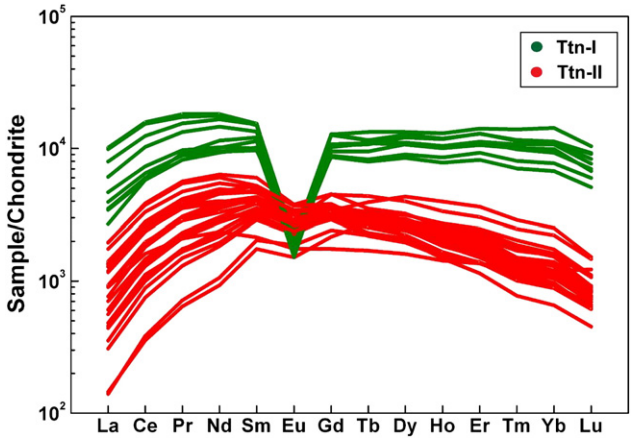

Fig. 6. Chondrite-normalized REE pattern of titanite from UHP granitic orthogneiss at Shuanghe in the Dabie orogen. Ttn-I domains denote the residual cores, and Ttn-II domains denote the newly grown rims or grains.

Table 5 (*continued*)

Spot	11-2-core	14-1n	S14-2n	14-3n	15-2n	15-3n	18-2n	19-1n	22-2n	22-3n	22-4n	25-1n
Rare earth elements (ppm)												
La	965	322	291	86	330	112	313	226	187	227	137	481
Ce	4142	1637	1542	566	1790	681	1703	1198	1157	1261	852	2390
Pr	852	362	341	144	401	169	393	280	280	275	211	525
Nd	4489	1897	1845	925	2337	1048	2172	1741	1672	1560	1313	2861
Sm	1492	593	604	460	713	483	737	621	643	587	547	804
Eu	137	151	164	139	194	138	193	173	164	174	153	214
Gd	1762	595	616	594	686	627	748	685	727	668	657	778
Tb	298	82.3	86.6	94.7	110	99.0	108	118	111	95.1	102	105
Dy	2154	499	533	612	633	663	666	702	696	567	653	624
Ho	443	86.6	91.3	108	109	120	116	127	121	94.1	116	104
Er	1364	225	231	270	267	302	285	322	302	229	299	256
Tm	181	27.7	26.4	30.6	31.1	35.3	31.4	38.5	32.7	25.8	33.5	28.3
Yb	1113	197	155	172	173	196	178	230	178	146	183	154
Lu	129	31.0	16.2	19.0	17.6	21.3	18.4	23.0	17.6	15.6	19.7	16.8
REE	19,522	6707	6543	4220	7791	4694	7662	6484	6288	5924	5276	9340
Trace elements (ppm)												
Sr	675	1048	1040	893	1137	806	1098	1094	1229	1139	945	1102
Ta	176.8	59.1	50.1	51.1	52.6	66.7	63.8	64.8	67.1	61.4	57.4	57.1
Nb	2014	1242	803	842	866	1009	935	1014	998	1346	895	864
Th	75.4	49.3	44.4	14.9	78.3	24.9	50.2	52.2	46.2	28.2	28.7	73.8
U	61.7	42.7	36.2	58.0	71.5	64.7	69.6	60.7	79.5	43.6	77.7	58.4
Pb	25.2	44.6	29.8	12.2	43.3	17.0	39.5	34.2	28.0	28.4	19.4	49.1
Zr	351.3	124.5	24.7	26.5	29.4	36.9	33.6	30.0	31.8	33.0	32.7	30.9
P	82.3	90.2	98.6	35.8	47.9	101.6	65.1	84.0	12.8	29.5	26.0	20.6
Y	12,170	2435	2488	2921	2964	3226	3133	3481	3324	2625	3196	2893
Hf	41.05	7.77	2.84	2.13	2.40	3.70	2.43	4.04	2.18	5.30	2.09	2.18
V	99.7	28.6	90.3	37.4	15.1	23.2	16.1	31.8	14.5	53.7	12.0	17.4
W	4.34	22.81	6.32	2.58	5.07	3.92	4.54	3.81	3.56	5.86	2.36	7.38
Lu/Hf	3.15	3.99	5.71	8.92	7.35	5.76	7.58	5.70	8.07	2.94	9.42	7.70
Nb/Ta	11.39	20.99	16.04	16.46	16.47	15.14	14.67	15.66	14.86	21.91	15.59	15.12
Eu/Eu*	0.26	0.78	0.82	0.81	0.85	0.76	0.80	0.81	0.74	0.85	0.78	0.83
$(Gd/Lu)_N$	1.69	2.39	4.72	3.89	4.83	3.65	5.05	3.70	5.13	5.33	4.15	5.76

Domains Ttn-I and Ttn-II have very different trace element features (Table 3 and Figs. 6 and 7). The REE distribution of domains Ttn-I is characterized by high REE contents (19,522 to 36,780 ppm), distinct negative Eu anomalies ($Eu/Eu^* = 0.12$ to 0.26), no MREE–HREE fractionations and flat HREE patterns with $(Gd/Lu)_N$ of 1.23 to 1.69. These domains also have high HFSE contents (e.g., Nb: 1367 to 2821 ppm; Zr: 213 to 954 ppm), high contents of Th (67.6 to 215 ppm) and U (52.4 to 124 ppm), and high Th/U ratios of 1.43 to 2.37. In contrast, domains Ttn-II have relatively low REE contents (2784 to 10,359 ppm), slightly negative Eu anomalies ($Eu/Eu^* = 0.59$ to 0.91), weak MREE–HREE fractionations and HREE-depleted patterns with $(Gd/Lu)_N$ of 1.90 to 5.83. These domains have relatively low HFSE contents (e.g., Nb: 556 to 1405 ppm; Zr: 24.7 to 125 ppm), low contents of Th (4.5 to 78.3 ppm) and U (30.7 to 83.6 ppm), and low Th/U ratios of 0.11 to 1.31 with an average of 0.72.

4.4. Zr-in-titanite geothermometry

Temperatures were calculated using the pressure-dependent Zr-in-titanite geothermometer of Hayden et al. (2008) at 0.5 to 1.0 GPa for analyses on domains Ttn-I and at 1.5 to 2.0 GPa for analyses on domains Ttn-II (Table 6), assuming the activity of unity for both TiO_2 (a_{TiO2}) and SiO_2 (a_{SiO2}). Accordingly, Zr contents of 213 to 954 ppm for domains Ttn-I correspond to Zr-in-titanite temperatures of 727–813 °C at 0.5 GPa and 785–877 °C at 1.0 GPa; those of 24.7 to 125 ppm for domains Ttn-II gave temperatures of 729–813 °C at 1.5 GPa and 782–870 °C at 2.0 GPa (Fig. 8). Because of the absence of rutile inclusion in domains Ttn-I, the activity of TiO_2 cannot be assumed as unity during their growth. Thus, the calculated temperatures could reduce by about 50–70 °C (Hayden et al., 2008). As a result, this type of titanites may grow at about 675 to 810 °C.

The X_{Al} values of 0.16 to 0.23 are obtained for domains Ttn-II (Table 4). They fall within the range of low-Al titanite (Oberti et al., 1991) and are lower than the minimum Al content of titanite in UHP metamorphic rocks from the Dabie orogen (Carswell et al., 1996). Thus, the metamorphic titanite was probably formed at HP rather than UHP conditions though low-Al titanites can sometimes form at UHP conditions (Ye et al., 2002). This is the reason why the Zr-in-titanite temperatures for Ttn-II domains are estimated at the pressures of 1.5 to 2.0 GPa. The rutile inclusions are occasionally found in domains Ttn-II, suggesting that the activity of TiO_2 can be assumed as unity during their growth.

5. Discussion

5.1. Magmatic vs. metamorphic titanite

5.1.1. Magmatic titanite

The titanite grains of domains Ttn-I are of magmatic origin on the basis of the following three criteria. First, they have profoundly low CaO and TiO_2 contents, high Fe_2O_3, Na_2O and MgO contents (Fig. 5), high REE and HFSE contents (Fig. 6) and remarkably negative Eu anomalies with flat MREE–HREE patterns, and high Th/U ratios. These features are consistent with the magmatic origin (e.g., Storey et al., 2007). Second, the petrographic observation indicates that domains Ttn-I contain inclusions of quartz and allanite (Fig. 3), which are different from the occasionally found inclusions of epidote, rutile and phengite in domains Ttn-II that are a HP metamorphic origin. Third, the U–Pb dating on domains Ttn-I gave the Neoproterozoic ages of 553 ± 28 to 689 ± 21 Ma (Fig. 4 and Table 3), which are younger than, but close to, zircon U–Pb ages of 724 ± 22 to 768 ± 22 Ma for protolith of the granitic orthogneiss at Shuanghe (Zheng et al., 2003b, 2005b,

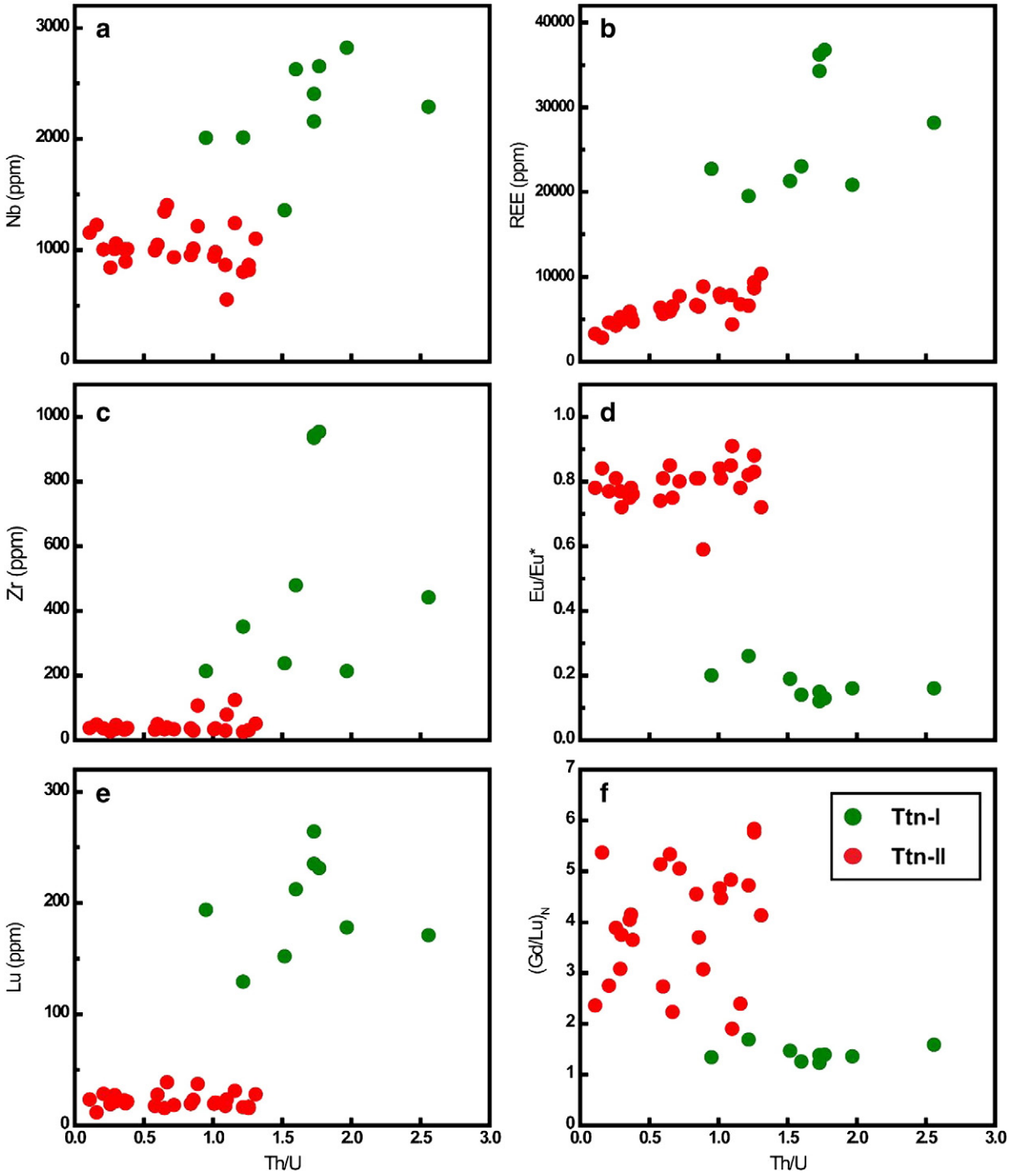

Fig. 7. Plots of Th/U vs. other major or trace elements for two groups of titanites from UHP metagranite at Shuanghe in the Dabie orogen. Ttn-I domains denote the residual cores, and Ttn-II domains denote the newly grown rims or grains.

2006). Although the high contents of common Pb limit the accuracy and reliability of titanite U–Pb ages (Horstwood et al., 2003; Simonetti et al., 2006; Storey et al., 2006, 2007), the Neoproterozoic U–Pb dates are consistent with the above conclusion that domains Ttn-I are of magmatic origin. In this regard, the oldest U–Pb age may be interpreted as an approximate to the time of titanite crystallization from granitic magma during its Neoproterozoic emplacement. The occurrence of allanite inclusions in domains Ttn-I indicates that there were relatively high REE contents in the granitic magma during the titanite growth.

An experimental study suggested that titanite is not stable in basaltic rocks at high P–T conditions (e.g., Liu et al., 1996). On the other hand, the survival of magmatic titanite in the Dabie UHP metagranite clearly indicates that titanite is stable in felsic rocks under continental subduction-zone HP–UHP conditions. Along the prograde and retrograde P–T path of a subduction-zone metamorphic rock, especially of eclogite and mafic granulite, titanite is commonly replaced by rutile at increasing pressure and transforms into titanite again during retrogression. These processes are often accompanied by hydration of HP to UHP assemblage at amphibolite-facies conditions (e.g., Brewer et al., 2003; Lucassen et al., 2010; Romer and Rötzler, 2003; Rötzler et al., 2004). Thus, the stability of magmatic titanite is principally dictated by mineralogical reactions in response to P–T changes and fluid action on the UHP mineral assemblages during the metamorphism.

Table 6
Zr-in-titanite temperatures for granitic orthogneiss in the Dabie orogen.

Spot	Zr (ppm)	0.5 GPa	1.0 GPa	1.5 GPa	2.0 GPa	2.5 GPa	3.0 GPa
Relict core							
5-1-core	935	812	875				
5-2-core	213	727	785				
5-3-core	441	767	828				
9-4-core	238	732	791				
9-5-core	479	771	833				
9-6-core	213	727	785				
11-2-core	351	754	814				
11-3-core	954	813	877				
11-4-core	942	812	876				
New growth							
1-1n	30.7			740	793	846	899
1-2n	37.0			749	802	856	910
1-3n	33.5			744	797	851	904
5-4-rim	35.8			747	801	854	908
5-5-rim	78.6			788	843	899	955
7-1n	38.8			751	805	859	913
8-1n	50.0			764	818	873	927
8-2n	107			804	861	917	974
8-3n	33.4			744	797	851	904
9-1-rim	32.1			742	795	848	902
9-2-rim	50.1			764	819	873	927
9-3-rim	47.5			761	816	870	924
9-7-rim	47.2			761	815	870	924
11-1-rim	35.9			747	801	854	908
14-1n	124			813	870	927	984
14-2n	24.7			729	782	834	887
14-3n	26.5			733	785	838	891
15-2n	29.4			738	791	844	897
15-3n	36.9			749	802	856	910
18-2n	33.6			744	798	851	904
19-1n	30.0			739	792	845	898
22-1n	36.0			748	801	855	908
22-2n	31.8			742	795	848	901
22-3n	33.0			743	797	850	903
22-4n	32.7			743	796	849	903
25-1n	30.9			740	793	846	900

Notes: Zr-in-titanite temperatures were calculated following the calibration of Hayden et al. (2008).

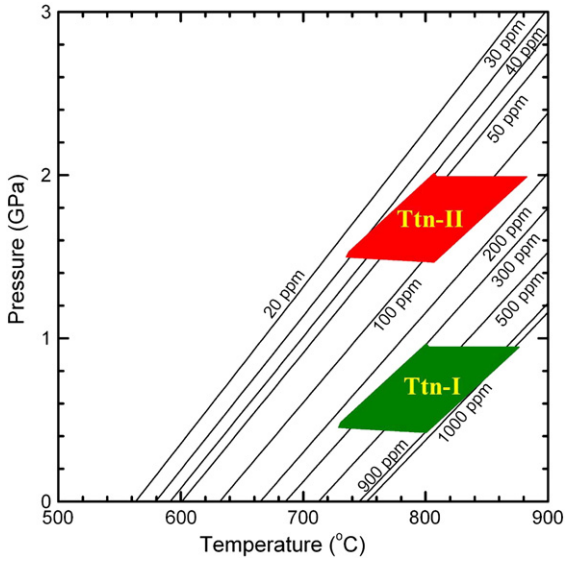

Fig. 8. Diagram of titanite Zr isopleths as a function of both temperature and pressure (calculated after the experimental calibration of Hayden et al., 2008). The areas Ttn-I (green) and Ttn-II (red) denote the Zr-in-titanite temperatures for two groups of titanites from UHP granitic orthogneiss at Shuanghe in the Dabie orogen.

5.1.2. Metamorphic titanite

Compared to domains Ttn-I that are interpreted as the magmatic origin, domains Ttn-II are interpreted as metamorphic origin based on the following three considerations. First, domains Ttn-II texturally occur as overgrown rims of dark BSE surrounding the magmatic cores and as grains of homogeneously dark BSE. They contain inclusions of HP metamorphic minerals, including not only hydrous minerals such as phengite, biotite and epidote but also nominally anhydrous minerals such as quartz, rutile and K-feldspar. Second, domains II have profoundly high contents of CaO and TiO_2 but low contents of Fe_2O_3, MgO and Al_2O_3, pointing to metamorphic growth. They have X_{Al} values falling within the range of low-Al metamorphic titanites (Oberti et al., 1991). They exhibit relatively low REE and HFSE contents (Fig. 6), slightly negative Eu anomalies with HREE-depleted patterns of REE distribution, and low Th/U ratios. These features are consistent with the metamorphic origin (e.g., Li et al., 2010; Storey et al., 2007). Third, the U–Pb dating of these domains gave the Triassic $^{206}Pb/^{238}U$ ages of 216 ± 4 Ma (Fig. 4 and Table 3). Despite large uncertainties, they are consistent with the zircon U–Pb ages of 215 ± 17 to 228 ± 12 Ma for the continental subduction-zone metamorphism (Zheng et al., 2003b, 2005b, 2006). Therefore, domains Ttn-II would grow during the Triassic continental collision, principally in the stage of decompression exhumation from HP eclogite-facies to amphibolite-facies with reference to known geochronological framework for the Dabie–Sulu UHP metamorphic rocks (Liu and Liou, 2011; Zheng et al., 2009). Nevertheless, the relatively uniform major element contents for these domains indicate that these titanites may grow from relatively homogeneous media. The Zr-in-titanite temperatures are 729–870 °C at 1.5–2.0 GPa, which are higher the Fe–Mg partition temperatures of 700–750 °C at the peak UHP conditions (Carswell et al., 1997; Cong et al., 1995; Okay, 1993). This suggests their growth in the stage of "hot" exhumation (Zhao et al., 2007; Gao et al., 2011), principally a product of retrograde metamorphism towards the amphibolite facies. This is consistent with fluid action in the continental subduction zone that is characterized by metamorphic dehydration and partial melting during exhumation of the deeply continental crust (Zheng et al., 2003a, 2009; Zhao et al., 2007; Xia et al., 2008, 2010; Zheng, 2009).

There are significant differences in trace element composition between the metamorphic and magmatic titanites (Figs. 6 and 7). They can be ascribed to the substitution of such elements as (1) REE, Y, Sr, U, Th, and Pb on the Ca site, and (2) HFSE (Nb, Ta, Zr, and W) on the Ti site. It was reported that few of these elements can sometimes reach unusually high concentrations: ZrO_2 up to 6 wt.% in magmatic titanite (e.g., Seifert and Kramer, 2003); Ta_2O_5 and Nb_2O_5 in pegmatitic titanite with 6 and 5 wt.%, respectively (Groat et al., 1985); Nb_2O_5 up to ~10 wt.% in metamorphic titanite (e.g., Bernau and Franz, 1987); combined Nb_2O_5 with ZrO_2 of 16 and 9 wt.%, respectively (Liferovich and Mitchell, 2005). The extremely high contents of these trace elements suggest that their incorporation is controlled by availability rather than compatibility. As a consequence, the content of trace elements, their distribution pattern and elemental ratios of chemically similar elements in titanite depends on both availability and compatibility of these trace elements during metamorphic dehydration, partial melting, and fractional crystallization in association with the mineralogical transformation from one Ti-phase to the other. Therefore, the differences in the trace element composition between the magmatic and metamorphic titanites are a manifestation of contrasts between magmatic melt and metamorphic fluid.

5.2. The preservation of primary Zr and Pb signatures in titanite

It is known that rates of element diffusion in minerals are a function of grain size and temperature. Thus, the occurrence of accessory minerals as matrix or inclusion in rock-forming minerals influences the element diffusivity and their potential loss by diffusion. Thus, it

is intriguing whether titanite has preserved its primary records of Zr and Pb after its initial growth and thus survived the UHP eclogite-facies metamorphism during continental collision. This issue can be addressed from the relationship that the distance of element diffusion across spherical grains is a function of diffusion coefficient and time (Crank, 1975):

$$r \approx \sqrt{Dt}$$

where r is the effective diffusion radius, t is the time and D is the diffusion coefficient that is available for Zr from the experimental determination of Cherniak (2006) and for Pb from the empirical calculation of Zhao and Zheng (2007).

By taking grain radii of 1, 10, 100 and 1000 μm as the effective diffusion radii, we made an estimate for timescales of achieving 100% loss at different temperatures. The results are illustrated in Fig. 9, in which curves represent the maximum duration by which the primary Zr and Pb signatures in titanite of different grain sizes (0.01 cm and 0.1 cm) cannot be preserved due to retrograde alteration at 600 to 1200 °C (Fig. 9a) or the minimum time–temperature conditions under which either the primary Zr and Pb signatures in titanite with grain radii from 1 to 1000 μm can be changed at 700 °C and 800 °C due to diffusion loss (Fig. 9b). The diffusion rates of Zr and Pb in titanite are so sluggish at 800 °C that complete resetting of Zr and Pb in titanite requires ~4 Myr for small titanite in a grain size of 100 μm and ~16 Myr for a grain size of 200 μm. For the inclusion titanite and the larger sizes of titanite (>100 μm), it appears that the diffusion is not an efficient mechanism to change its Zr and Pb contents during the HP/UHP metamorphism in the Dabie orogen at temperatures up to 800 °C. If the experimental and calculated diffusion coefficients of Zr and Pb in titanite are applicable to nature, the primary Zr and Pb records of natural titanite, including the titanite Zr and Pb zoning, can survive short-lived (≤10 Myr) eclogite-facies recrystallization at elevated temperatures as high as 850 °C .

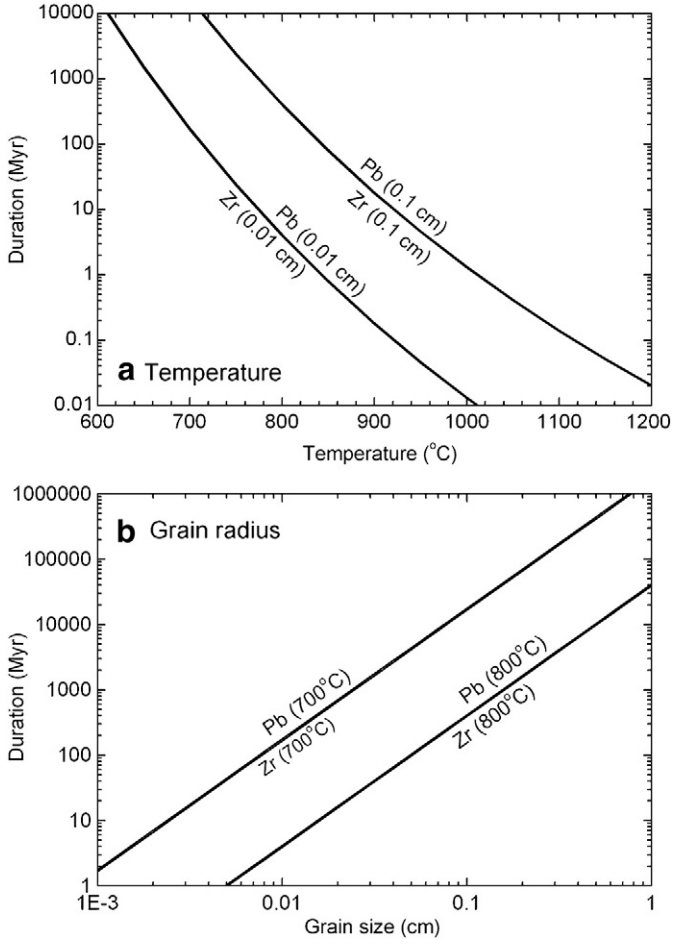

Fig. 9. Timescale for diffusion resetting of Zr and Pb in titanite at different temperatures or grain sizes. (a) The maximum time–temperature conditions under which the primary Zr and Pb signature in titanite with grain radii of 100 to 1000 μm cannot be preserved due to diffusion resetting; (b) the minimum duration by which the primary Zr and Pb signature in titanite of different grain sizes can be changed due to retrograde alteration at temperatures of 700 and 800 °C. Diffusion coefficients after Cherniak (2006) for Zr and Zhao and Zheng (2007) for Pb.

5.3. The closure temperature of Pb diffusion in titanite

To know the closure temperature of titanite U–Pb system is useful for interpretation of its U–Pb age. However, estimation of the closure temperature for titanite U–Pb chronometric system is complex (Frost et al., 2000). This problem is partly caused by the fact that the closure temperature is a complex function involving element diffusivity (D) and effective diffusion radius, as well as cooling rate of geological targets (Dodson, 1973).

In slowly cooling high-grade metamorphic terranes, titanite U–Pb ages are usually interpreted as the effective cease of Pb diffusion at a given temperature (Tc), whereas in rapidly cooling igneous bodies, titanite U–Pb ages can be used to approximate the timing of magma intrusion (Jung and Hellebrand, 2007). Early estimates of Tc for small grains of titanites based on slowly cooling natural samples were ca. 600 °C (Heaman and Parrish, 1990; Mezger et al., 1991; Tucker et al., 1986). Scott and St-Onge (1995) suggested that the closure temperature of Pb diffusion in titanite is probably higher than 660–700 °C. However, the inherited Pb component was detected in titanite from syenites (Pidgeon et al., 1996; Zhang and Schärer, 1996), indicating that Pb retentivity at the temperatures of high-grade metamorphism or crustal anatexis. Therefore, a closure temperature of >650 °C was proposed for the titanite U–Pb chronometric system. Studies on contact metamorphic rocks indicated that titanite was completely reset at temperatures >700 °C (Verts et al., 1996), suggesting that the closure temperature in this case is not far above 700 °C. Based on experimentally measured Pb diffusion parameters by Cherniak (1993), closure temperatures of ca. 660 °C, ca. 630 °C and ca. 600 °C are estimated for grain sizes between 0.1 and 0.2 mm and cooling rates of 100 °C/Ma, 100 °C/Ma, 2 °C/Ma, respectively. Therefore, in slowly cooling terranes, titanite U–Pb ages may probably record cooling ages during the waning stages of metamorphism,

The titanite U–Pb data obtained in this study provide evidence of a rather high closure temperature for the titanite U–Pb system. The 689 ± 21 Ma age was obtained on domain Ttn-I, the bright core in some grains. The textural and chemical results indicate that this type of domains is inherited from the granitic protolith. The inherited magmatic titanite survived the continental subduction-zone HP–UHP metamorphism with temperatures as high as 800–850 °C in the Dabie orogen (Carswell et al., 1997; Cong et al., 1995; Gao et al., 2011). The other two domains are characterized by the metamorphic Pb loss resulting in younger U–Pb ages (Fig. 4). The observation that the magmatic titanites survived the elevated temperatures during the HP–UHP metamorphism suggests that the closure temperature of U–Pb system in titanite may exceed at least 800 °C (or possibly up to 850 °C).

6. Conclusions

Relict magmatic titanite is identified in the cores of bright BSE from a few titanite grains in the mid-T/UHP granitic orthogneiss in the Dabie orogen, with metamorphic titanite as rims and grains of homogeneously dark BSE. LA–ICPMS U–Pb dating gave Neoproterozoic ages for the magmatic cores but Triassic ages for the metamorphic rims and grains. The magmatic and metamorphic titanites are clearly distinguished from each other by the differences in petrological and geochemical compositions. The magmatic titanite contains the inclusions

of allanite and quartz, and is characterized by profoundly lower contents of CaO, Al_2O_3 and TiO_2, and remarkably higher contents of Fe_2O_3 and MgO, compared to the metamorphic titanite. The metamorphic titanite contains the inclusions of epidote, quartz, biotite, K-feldspar, rutile and phengite. In trace elements, the magmatic titanite shows significantly high REE and HFSE contents, distinctly negative Eu anomalies with flat MREE–HREE patterns, and high Th/U ratios. In contrast, the metamorphic titanite exhibits relatively low REE and HFSE contents, slightly negative Eu anomalies with HREE depletion relative to MREE, and low Th/U ratios. Zr-in-titanite temperatures are 727 to 877 °C at 0.5 to 1.0 GPa for the magmatic titanite, and 729 to 870 °C at 1.5 to 2.0 GPa for the metamorphic titanite. It appears that the Neoproterozoic U–Pb chronometric system in the magmatic titanite survived the Triassic HP–UHP metamorphism during continental collision. This provides an important constraint on the closure temperature of Pb diffusion in titanite. The relatively high closure temperature of >800 °C is possible for the titanite U–Pb system. The metamorphic titanite was principally produced in the stage of decompression exhumation at the transition from HP eclogite-facies to amphibolite-facies. Therefore, there are polygenetic titanites in the UHP eclogite-facies metagranite, which can be used to decipher the chemical geodynamics in continental subduction-zones.

Acknowledgments

This study was supported by funds from the Chinese Ministry of Science and Technology (2009CB825004) and the Natural Science Foundation of China (40903015 and 40921002). Thanks are due to Yongsheng Liu for his assistance for LA–ICPMS analyses and to Shu Zheng for his assistance for EMP analysis. We are grateful to I. Buick, J.G. Liou and one anonymous reviewer for their comments that greatly help improvement of the presentation.

References

Aleinikoff, J.N., Wintsch, R.P., Tollo, R.P., Unruh, D.M., Fanning, C.M., Schmitz, M.D., 2007. Ages and origins of rocks of the Killingworth Dome, south-central Connecticut; implications for the tectonic evolution of southern New England. American Journal of Science 307, 63–118.

Amelin, Y., 2009. Sm–Nd and U–Pb systematics of single titanite grains. Chemical Geology 261, 53–61.

Bernau, R., Franz, G., 1987. Crystal chemistry and genesis of Nb-, V-, and Al-rich metamorphic titanite from Egypt and Greece. Canadian Mineralogist 25, 695–705.

Brewer, T.S., Storey, C.D., Parrish, R.R., Temperley, S., Windley, B.F., 2003. Grenvillian age decompression of eclogites in the Glenelg-Attadale Inlier, NW Scotland. Journal of the Geological Society 160, 565–574.

Buick, I.S., Hermann, J., Maas, R., Gibson, R.L., 2007. The timing of sub-solidus hydrothermal alteration in the Central Zone, Limpopo Belt (South Africa): constraints from titanite U–Pb geochronology and REE partitioning. Lithos 98, 97–117.

Carswell, D.A., Compagnoni, R., 2003. Ultra-high pressure metamorphism. European Mineralogical Union Notes 5, 1–508.

Carswell, D.A., Wilson, R.N., Zhai, M., 1996. Ultra-high pressure aluminous titanites in carbonate-bearing eclogites at Shuanghe in Dabieshan, central China. Mineralogical Magazine 60, 461–471.

Carswell, D.A., O'Brien, P.J., Wilson, R.N., Zhai, M.G., 1997. Thermobarometry of phengite-bearing eclogites in the Dabie Mountains of central China. Jounral of Metamorphic Geology 15, 239–252.

Chen, R.-X., Zheng, Y.-F., Gong, B., 2011. Mineral hydrogen isotopes and water contents in ultrahigh-pressure metabasite and metagranite: constraints on fluid flow during continental subduction-zone metamorphism. Chemical Geology 281, 103–124.

Cherniak, D.J., 1993. Lead diffusion in sphene and preliminary results on the effects of radiation damage on Pb transport. Chemical Geology 110, 177–194.

Cherniak, D., 2006. Zr diffusion in titanite. Contributions to Mineralogy and Petrology 152, 639–647.

Cong, B.L., 1996. Ultrahigh-Pressure Metamorphic Rocks in the Dabieshan–Sulu Region of China. Science Press, Beijing. 224 pp.

Cong, B.L., Zhai, M.G., Carswell, D.A., Wilson, R.N., Wang, Q.C., Zhao, Z.Y., Windley, B.F., 1995. Petrogenesis of ultrahigh-pressure rocks and their country rocks at Shuanghe in Dabieshan, Central China. European Journal of Mineralogy 7, 119–138.

Corfu, F., Stone, D., 1998. The significance of titanite and apatite U–Pb ages: constrains for the post-magmatic thermal–hydrothermal evolution of a batholitic complex, Berens River Area, northwest Superior Province, Canada. Geochimica et Cosmochimica Acta 62, 2979–2995.

Corfu, F., Krogh, T.E., Ayres, L.D., 1985. U–Pb zircon and sphene geochronology of a composite Archean granitoid batholith, Favourable Lake area, northwestern Ontario. Canadian Journal of Earth Sciences 22, 1436–1451.

Corfu, F., Heaman, L.M., Rogers, G., 1994. Polymetamorphic evolution of the Lewisian complex, NW Scotland, as recorded by U–Pb isotopic compositions of zircon, titanite and rutile. Contributions Mineralogy and Petrology 117, 215–228.

Crank, J., 1975. The Mathematics of Diffusion, 2nd Edition. Oxford University Press, Oxford. 414 pp.

Crowley, J.L., 2002. Testing the model of late Archean terrane accretion in southern West Greenland: a comparison of the timing of geological events across the Qarliit Nunaat Fault, Buksefjorden region. Precambrian Research 116, 57–79.

Dasgupta, S., 1993. Contrasting mineral parageneses in high-temperature calc-silicate granulites: examples from the Eastern Ghats, India. Journal of Metamorphic Geology 11, 193–202.

Dodson, M.H., 1973. Closure temperature in cooling geochronological and petrological systems. Contributions to Mineralogy and Petrology 40, 259–274.

Enami, M., Suzuki, K., Liou, J.G., Bird, D.K., 1993. Al–Fe^{3+} and F–OH substitutions in titanite and constraints on their P–T dependence. European Journal of Mineralogy 5, 219–231.

Ernst, W.G., 2005. Alpine and Pacific styles of Phanerozoic mountain building: subduction-zone petrogenesis of continental crust. Terra Nova 17, 165–188.

Force, E.R., 1991. Geology of titanium mineral deposits. Geological Society of America Special Paper 259, 1–120.

Franz, G., Spear, F.S., 1985. Aluminous titanite (sphene) from the eclogite zone, South-central Tauern Window, Austria. Chemical Geology 50, 33–46.

Frost, B.R., Chamberlain, K.R., Schumacher, J.C., 2000. Sphene (titanite): phase relations and role as a geochronometer. Chemical Geology 172, 131–148.

Fu, B., Zheng, Y.-F., Wang, Z.R., Xiao, Y.L., Gong, B.L., Li, S.G., 1999. Oxygen and hydrogen isotope geochemistry of gneisses associated with ultrahigh pressure eclogites at Shuanghe in the Dabie Mountains. Contributions to Mineralogy and Petrology 134, 52–66.

Fu, B., Touret, J.L.R., Zheng, Y.F., 2001. Fluid inclusions in coesite-bearing eclogites and jadeite quartzites at Shuanghe, Dabie Shan, China. Journal of Metamorphic Geology 19, 529–545.

Gao, X.-Y., Zheng, Y.-F., Chen, Y.-X., 2011. U–Pb ages and trace elements in metamorphic zircon and titanite from UHP eclogite in the Dabie orogen: constraints on *P–T–t* path. Journal of Metamorphic Geology 29, doi:10.1111/j.1525-1314.2011.00938.x.

Groat, L.A., Carter, R.T., Hawthorne, F.C., Ercitt, T.S., 1985. Tantalian niobian titanite from the Irgon Claim, southeastern Manitoba. Canadian Mineralogist 23, 569–571.

Gromet, P., Silver, L.T., 1983. Rare earth element distribution among minerals in granodiorite and their petrogenetic implications. Geochimica et Cosmochimica Acta 47, 925–939.

Harlov, D., Tropper, P., Seifert, W., Nijland, T., Förster, H., 2006. Formation of Al-rich titanite ($CaTiSiO_4O$–$CaAlSiO_4OH$) reaction rims on ilmenite in metamorphic rocks as a function of fH_2O and fO_2. Lithos 88, 72–84.

Hayden, L.A., Watson, E.B., Wark, D.A., 2008. A thermobarometer for sphene (titanite). Contributions to Mineralogy and Petrology 155, 529–540.

Heaman, L.M., 2009. The application of U–Pb geochronology to mafic, ultramafic and alkaline rocks: an evaluation of three mineral standards. Chemical Geology 261, 42–51.

Heaman, L., Parrish, R., 1990. U–Pb geochronology in accessory minerals. Short Course of the Mineralogical Association of Canada, 19, pp. 59–102.

Hirajima, T., Zhang, R., Li, J., Cong, B., 1992. Petrology of nyböite-bearing eclogite in the Donghai area, Jiangsu province, eastern China. Mineralogical Magazine 56, 37–49.

Horstwood, M.S.A., Foster, G.L., Parrish, R.R., et al., 2003. Common-Pb corrected in situ U–Pb accessory mineral geochronology by LA–MC–ICP-MS. Journal of Analytical Atomic Spectrometry 18, 837–846.

Jung, S., Hellebrand, E., 2007. Textural, geochronological and chemical constraints from polygenetic titanite and monogenetic apatite from a mid-crustal shear zone: an integrated EPMA, SIMS, and TIMS study. Chemical Geology 241, 88–107.

Kinny, P.D., McNaughton, N.J., Fanning, C.M., et al., 1994. 518 Ma sphene (titanite) from the Khan pegmatite, Namibia, southwest Africa: a potential ion-microprobe standard. Abstracts of ICOG8 at Berkeley: US Geological Survey Circular 1107, p. 171.

Kylander-Clark, A.R.C., Hacker, B.R., Mattinson, J.M., 2008. Slow exhumation of UHP terranes: titanite and rutile ages of the Western Gneiss Region, Norway. Earth and Planetary Science Letters 272, 531–540.

Li, S.G., Jagoutz, E., Lo, C.H., Chen, Y., Li, Q., Xiao, Y., 1999. Sm/Nd, Rb/Sr, and $^{40}Ar/^{39}Ar$ isotopic systematics of the ultrahigh-pressure metamorphic rocks in the Dabie–Sulu Belt, Central China; a retrospective view. International Geology Review 41, 1114–1124.

Li, S.G., Jagoutz, E., Chen, Y.Z., Li, Q.L., 2000. Sm–Nd and Rb–Sr isotopic chronology and cooling history of ultrahigh pressure metamorphic rocks and their country rocks at Shuanghe in the Dabie Mountains, Central China. Geochimica et Cosmochimica Acta 64, 1077–1093.

Li, J.W., Deng, X.D., Zhou, M.F., Liu, Y.S., Zhao, X.F., Guo, J.L., 2010. Laser ablation ICP-MS titanite U–Th–Pb dating of hydrothermal ore deposits: a case study of the Tonglushan Cu–Fe–Au skarn deposit, SE Hubei Province, China. Chemical Geology 270, 56–67.

Liferovich, R.L., Mitchell, R.H., 2005. Composition and paragenesis of Na-, Nb- and Zr-bearing titanite from Khibina, Russia, and crystal-structure data for synthetic analogues. Canadian Mineralogist 43, 795–812.

Liou, J.G., Zhang, R.Y., Eide, E.A., Wang, X.M., Ernst, W.G., Maruyam, A.S., 1996. Metamorphism and tectonics of high-pressure and ultra-high-pressure belts in the Dabie Sulu region, China. In: Harrison, M.T., Yin, A. (Eds.), The Tectonics of Asia. Cambridge University Press, Cambridge, pp. 300–344.

Liou, J.G., Ernst, W.G., Zhang, R.Y., Tsujimori, T., Jahn, J.G., 2009. Ultrahigh-pressure minerals and metamorphic terranes — the view from China. Journal of Asian Earth Sciences 35, 199–231.

Liu, F.L., Liou, J.G., 2011. Zircon as the best mineral for P–T–time history of UHP metamorphism: a review on mineral inclusions and U–Pb SHRIMP ages of zircons from the Dabie–Sulu UHP rocks. Journal of Asian Earth Sciences 40, 1–39.
Liu, J., Bohlen, S.R., Ernst, W.G., 1996. Stability of hydrous phases in subducting oceanic crust. Earth and Planetary Science Letters 143, 161–171.
Liu, F.L., Gerdes, A., Liou, J.G., Xue, H.M., Liang, F.H., 2006. SHRIMP U–Pb zircon dating from Sulu–Dabie dolomitic marble, eastern China: constraints on prograde, ultrahigh-pressure and retrograde metamorphic ages. Journal of Metamorphic Geology 24, 569–589.
Liu, Y.S., Hu, Z.C., Gao, S., Günther, D., Xu, J., Gao, C.G., Chen, H.H., 2008. In situ analysis of major and trace elements of anhydrous minerals by LA–ICP-MS without applying an internal standard. Chemical Geology 257, 34–43.
Liu, Y.S., Gao, S., Hu, Z.C., Gao, C.G., Zong, K.Q., Wang, D.B., 2010. Continental and oceanic crust recycling-induced melt-peridotite interactions in the Trans-North China Orogen: U–Pb dating, Hf isotopes and trace elements in zircons of mantle xenoliths. Journal of Petrology 51, 537–571.
Lucassen, F., Dulski, P., Abart, R., Franz, G., Rhede, D., Romer, R.L., 2010. Redistribution of HFSE elements during rutile replacement by titanite. Contributions to Mineralogy and Petrology 160, 279–295.
Manning, C.E., Bohlen, S.R., 1991. The reaction titanite + kyanite = anorthite + ruffle and titaniterutile barometry in eclogites. Contributions to Mineralogy and Petrology 109, 1–9.
Mattinson, J.M., 1986. Geochronology of high pressure–low temperature Franciscan metabasites: a new approach using the U–Pb system. In: Evans, B.W., Brown, E.H. (Eds.), Blueschists and Eclogites: Geological Society of America Memoir, 164, pp. 95–105.
Mattinson, J.M., Echeverria, L.M., 1980. Ortigalita Peak gabbro, Franciscan Complex: U–Pb ages of intrusion and high pressure–low temperature metamorphism. Geology 8, 589–593.
Mezger, K., Rawnsley, C.M., Bohlen, S.R., Hanson, G.N., 1991. U–Pb garnet, sphene, monazite, and rutile ages: implications for the duration of high-grade metamorphism and cooling histories, Adirondack Mts, New York. The Journal of Geology 99, 415–428.
Mezger, K., Essene, E.J., van der Pluijm, B.A., Halliday, A.N., 1993. U–Pb geochronology of the Grenville Orogen of Ontario and New York: constraints on ancient crustal tectonics. Contributions to Mineralogy and Petrology 114, 13–26.
Motoyoshi, Y., Thost, D.E., Hansen, B.J., 1991. Reaction textures in calc-silicate granulites from the Bolingen Islands, Prydz Bay, East Antarctica: implications for the retrograde P–T path. Journal of Metamorphic Geology 9, 293–300.
Nemchin, A.A., Pidgeon, R.T., 1999. U–Pb ages on titanite and apatite from the Darling Range granite: implications for Late Archaean history of the southwestern Yilgarn Craton. Precambrian Research 96, 125–139.
Oberti, R., Smith, D.C., Rossi, G., Caucia, F., 1991. The crystal-chemistry of high-aluminum titanites. European Journal of Mineralogy 3, 777–792.
Okay, A.I., 1993. Petrology of a diamond and coesite-bearing metamorphic terrain: Dabie Shan, China. European Journal of Mineralogy 5, 659–673.
Okay, A.I., Xu, S.T., Sengor, A.M.C., 1989. Coesite from the Dabie Shan eclogites, central China. European Journal of Mineralogy 1, 595–598.
Pidgeon, R.T., Bosch, D., Bruguier, O., 1996. Inherited zircon and titanite U–Pb systematics in an Archean syenite from southwestern Australia: implications for U–Pb stability of titanite. Earth and Planetary Science Letters 141, 187–198.
Romer, R.L., Rötzler, J., 2003. Effect of metamorphic reaction history on the U–Pb dating of titanite. In: Vance, D. (ed.), Geochronology: Linking the Isotopic Record with Petrology and Textures. Geological Society Special Paper 220, 147–158.
Rötzler, J., Romer, R.L., Budzinski, H., Oberhänsli, R., 2004. Ultrahigh-temperature granulites from Tirschheim, Saxon Granulite Massif, Germany: P–T–t path and geotectonic implications. European Journal of Mineralogy 16, 917–937.
Schertl, H., Okay, A.I., 1994. Coesite inclusion in dolomite of Dabie Shan, China: petrological and geological significance. European Journal of Mineralogy 6, 995–1000.
Schmitz, M.D., Bowring, S.A., 2001. U–Pb zircon and titanite systematics of the Fish Canyon Tuff: an assessment of high-precision U–Pb geochronology and its application to young volcanic rocks. Geochimica et Cosmochimica Acta 65, 2571–2587.
Scott, D.J., St-Onge, M.R., 1995. Constraints on Pb closure temperature in sphene based on rocks from the Ungava orogen, Canada: implications for geochronology and P–T–t path determinations. Geology 23, 1123–1126.
Seifert, W., Kramer, W., 2003. Accessory titanite: an important carrier of zirconium in lamprophyres. Lithos 71, 81–98.
Simonetti, A., Heaman, L.M., Chacko, T., Banerjee, N.R., 2006. In situ petrographic thin section U-Pb dating of zircon, monazite, and titanite using laser ablation-MC-ICP-MS. Internal Journal of Mass Spectrometry 253, 87–97.
Smith, D.C., 1977. Aluminum bearing sphene in eclogites from Sunnmore (Norway). Geology 10, 32–33.
Sobolev, N.V., Shatsky, V.S., 1990. Diamond inclusions in garnets from metamorphic rocks: a new environment for diamond formation. Nature 343, 742–746.
Stacey, J.S., Kramers, J.D., 1975. Approximation of terrestrial lead isotope evolution by a two-stage model. Earth and Planetary Science Letters 26, 207–221.
Storey, C.D., Jeffries, T.E., Smith, M., 2006. Common lead-corrected laser ablation ICP-MS U–Pb systematics and geochronology of titanite. Chemical Geology 227, 37–52.
Storey, C.D., Smith, M.P., Jeffries, T.E., 2007. In situ LA–ICP-MS U–Pb dating of metavolcanics of Norrbotten, Sweden: records of extended geological histories in complex titanite grains. Chemical Geology 240, 163–181.
Sun, S.-s., McDonough, W.F., 1989. Chemical and isotope systematics of oceanic basalt: implications for mantle composition and processes. In: Sanders, A.D., Norry, M.J. (Eds.), Magmatism in the Ocean Basins: Geological Society Special Publication 42, pp. 313–345.
Tiepolo, M., Oberti, R., Vannucci, R., 2002. Trace-element incorporation in titanite: constraints from experimentally determined solid/liquid partition coefficients. Chemical Geology 191, 105–119.
Tilton, G.R., Grunenfelder, M.H., 1968. Sphene: uranium–lead ages. Science 159, 1458–1461.
Tsai, C.H., Liou, J.G., 2000. Eclogite-facies relics and inferred ultrahigh-pressure metamorphism in the North Dabie Complex, central-eastern China. American Mineralogist 85, 1–8.
Tucker, R.D., Raheim, A., Krogh, T.E., Corfu, F., 1986. Uranium–lead zircon and titanite ages from the northern portion of the Western Gneiss Region, south-central Norway. Earth and Planetary Science Letters 81, 203–211.
Tucker, R.D., Robinson, P., Solli, A., Gee, D.G., Thorsnes, T., Krogh, T.E., Nordgulen, Ø., Bickford, M.E., 2004. Thrusting and extension in the Scandian hinterland, Norway: new U–Pb ages and tectonostratigraphic evidence. American Journal of Science 304, 477–532.
Verts, L.A., Chamberlain, K.R., Frost, C.D., 1996. U–Pb sphene dating of metamorphism: the importance of sphene growth in the contact aureole of the Red Mountain pluton, Laramie Mountains, Wyoming. Contributions to Mineralogy and Petrology 125, 186–199.
Wang, X.M., Liou, J.G., 1991. Regional ultra-pressure coesite-bearing eclogitic terrane in central China: evidence from country rocks, gneiss, marble, and metapelite. Geology 19, 933–936.
Wang, X.M., Liou, J.G., Mao, H.K., 1989. Coesite-bearing eclogite from the Dabie Mountains in central China. Geology 17, 1085–1088.
Wang, X.M., Liou, J.G., Maruyama, S., 1992. Coesite-bearing eclogites from the Dabie Mountains in central China: petrogenesis, P–T paths, and implications for regional tectonics. The Journal of Geology 139, 1–16.
Wang, X.M., Zhang, R.Y., Liou, J.G., 1995. UHPM terrane in east central China. In: Coleman, R., Wang, X.M. (Eds.), Ultrahigh Pressure Metamorphism. Cambridge University Press, Cambridge, pp. 356–390.
Whitney, D.L., Evans, B.W., 2010. Abbreviations for names of rock-forming minerals. American Mineralogist 95, 185–187.
Wu, Y.B., Zheng, Y.F., Zhao, Z.F., Gong, B., Liu, X.M., Wu, F.-Y., 2006. U–Pb, Hf and O isotope evidence for two episodes of fluid-assisted zircon growth in marble-hosted eclogites from the Dabie orogen. Geochimica et Cosmochimica Acta 70, 3743–3761.
Xia, Q.-X., Zheng, Y.-F., Zhou, L.-G., 2008. Dehydration and melting during continental collision: constraints from element and isotope geochemistry of low-T/UHP granitic gneiss in the Dabie orogen. Chemical Geology 247, 36–65.
Xia, Q.-X., Zheng, Y.-F., Hu, Z.-C., 2010. Trace elements in zircon and coexisting minerals from low-T/UHP metagranite in the Dabie orogen: implications for fluid regime during continental subduction-zone metamorphism. Lithos 114, 385–413.
Xiao, Y.L., Hoefs, J., van den Kerkhof, A.M., Li, S.G., 2001. Geochemical constraints of the eclogite and granulite facies metamorphism as recognized in the Raobazhai complex from North Dabie Shan, China. Journal of Metamorphic Geology 19, 3–19.
Xu, S.T., Okay, A.I., Ji, S.Y., Sengor, A.M.C., Su, W., Liu, Y.C., Jiang, L.L., 1992. Diamond from the Dabie Shan metamorphic rocks and its implication for tectonic setting. Science 256, 80–82.
Xu, S.T., Liu, Y.C., Chen, G.B., Roberto, C., Franco, R., He, M.C., Liu, H.F., 2003. New finding of microdiamonds in eclogites from Dabie–Sulu region in central-eastern China. Chinese Science Bulletin 48, 988–994.
Xu, S.T., Liu, Y.C., Chen, G.B., Ji, S.Y., Ni, P., Xiao, W.S., 2005. Microdiamonds, their classification and tectonic implications for the host eclogites from the Dabie and Sulu regions in central eastern China. Mineralogical Magazine 69, 509–520.
Ye, K., Ye, D.N., 1996. Significance of phosphorous (P) and magnesium (Mg)-bearing high-Al titanite in high-pressure marble from Yangguantun, Rongcheng County, Shandong Province. Chinese Science Bulletin 41, 1194–1197.
Ye, K., Liu, J.B., Cong, B.L., Ye, D.N., Xu, P., Omori, S., Maruyama, S., 2002. Ultrahigh-pressure (UHP) low-Al titanites from carbonate-bearing rocks in Dabieshan–Sulu UHP terrane, eastern China. American Mineralogist 87, 875–881.
Zadnik, M.G., Specht, S., Begemann, F., 1989. Revised isotopic composition of terrestrial mercury. International Journal of Mass Spectrometer & Ion Processes 89, 103–110.
Zhang, L.-S., Schärer, U., 1996. Inherited Pb components in magmatic titanite and their consequences for the interpretation of U–Pb ages. Earth and Planetary Science Letters 138, 57–65.
Zhang, R.Y., Hirajima, T., Banno, S., Cong, B.L., Liou, J.G., 1995. Petrology of ultrahigh-pressure rocks from the southern Sulu region, eastern China. Journal of Metamorphic Geology 13, 659–675.
Zhang, R.Y., Liou, J.G., Zheng, Y.-F., Fu, B., 2003. Transition of UHP eclogites to gneissic rocks of low-grade amphibolite facies during exhumation: evidence from the Dabie terrane, central China. Lithos 70, 269–291.
Zhang, R.Y., Liou, J.G., Ernst, W.G., 2009. The Dabie–Sulu continental collision zone: a comprehensive review. Gondwana Research 16, 1–26.
Zhao, Z.-F., Zheng, Y.-F., 2007. Diffusion compensation for argon, hydrogen, lead, and strontium in minerals: empirical relationships to crystal chemistry. American Mineralogist 92, 289–308.
Zhao, Z.-F., Zheng, Y.-F., Gao, T.-S., Wu, Y.-B., Chen, B., Chen, F.K., Wu, F.-Y., 2006. Isotopic constraints on age and duration of fluid-assisted high-pressure eclogite-facies recrystallization during exhumation of deeply subducted continental crust in the Sulu orogen. Journal of Metamorphic Geology 24, 687–702.
Zhao, Z.-F., Zheng, Y.-F., Chen, R.-X., Xia, Q.-X., Wu, Y.-B., 2007. Element mobility in mafic and felsic ultrahigh-pressure metamorphic rocks during continental collision. Geochim. Cosmochim. Acta 71, 5244–5266.
Zheng, Y.F., 2008. A perspective view on ultrahigh-pressure metamorphism and continental collision in the Dabie–Sulu orogenic belt. Chinese Science Bulletin 53, 3081–3104.
Zheng, Y.F., 2009. Fluid regime in continental subduction zones: petrological insights from ultrahigh-pressure metamorphic rocks. Journal of the Geological Society 166, 763–782.
Zheng, Y.-F., Fu, B., Li, Y.-L., Xiao, Y.L., Li, S.G., 1998. Oxygen and hydrogen isotope geochemistry of ultrahigh pressure eclogites from the Dabie Mountains and the Sulu terrane. Earth and Planetary Science Letters 155, 113–129.

Zheng, Y.-F., Gong, B., Li, Y.-L., Wang, Z.-R., Fu, B., 2000. Carbon concentrations and isotopic ratios of eclogites from the Dabie and Sulu terranes in China. Chemical Geology 168, 291–305.
Zheng, Y.-F., Fu, B., Gong, B., Li, L., 2003a. Stable isotope geochemistry of ultrahigh pressure metamorphic rocks from the Dabie–Sulu orogen in China: implications for geodynamics and fluid regime. Earth Science Review 62, 105–161.
Zheng, Y.-F., Gong, B., Zhao, Z.-F., Fu, B., Li, Y.-L., 2003b. Two types of gneisses associated with eclogite at Shuanghe in the Dabie terrane: carbon isotope, zircon U–Pb dating and oxygen isotope. Lithos 70, 321–343.
Zheng, Y.-F., Zhou, J.-B., Wu, Y.-B., Xie, Z., 2005a. Low-grade metamorphic rocks in the Dabie–Sulu orogenic belt: a passive-margin accretionary wedge deformed during continent subduction. International Geology Review 47, 851–871.
Zheng, Y.-F., Wu, Y.-B., Zhao, Z.-F., Zhang, S.-B., Xu, P., Wu, F.Y., 2005b. Metamorphic effect on zircon Lu–Hf and U–Pb isotope systems in ultrahigh-pressure eclogite-facies metagranite and metabasite. Earth and Planetary Science Letters 240, 378–400.
Zheng, Y.-F., Zhao, Z.-F., Wu, Y.-B., Zhang, S.-B., Liu, X.-M., Wu, F.-Y., 2006. Zircon U-Pb age, Hf and O isotope constraints on protolith origin of ultrahigh-pressure eclogite and gneiss in the Dabie orogen. Chemical Geology 231, 135–158.
Zheng, Y.-F., Chen, R.-X., Zhao, Z.-F., 2009. Chemical geodynamics of continental subduction-zone metamorphism: insights from studies of the Chinese Continental Scientific Drilling (CCSD) core samples. Tectonophysics 475, 327–358.
Zheng, Y.-F., Gao, X.-Y., Chen, R.-X., Gao, T.S., 2011. Zr-in-rutile thermometry of eclogite in the Dabie orogen: constraints on rutile growth during continental subduction-zone metamorphism. Journal of Asian Earth Sciences 40, 427–451.